

Network Pharmacology and Experimental Verification: Phellodendri Chinensis Cortex-Cnidii Fructus Herb Pair Alleviates Atopic Dermatitis by Regulating the TLR4/NF- κ B Pathway

Xinyue Liu¹, Lele Chen¹, Peng Sun¹, Xiaolong Jiang¹, Pengze Li², Zichen Xu³, Zhaoshuang Zhan¹, Jiafeng Wang¹

¹College of Chinese Medicine, Shandong University of Traditional Chinese Medicine, Jinan, People's Republic of China; ²College of Medicine, Shandong University of Traditional Chinese Medicine, Jinan, People's Republic of China; ³College of Optometry and Ophthalmology, Shandong University of Traditional Chinese Medicine, Jinan, People's Republic of China

Correspondence: Zhaoshuang Zhan; Jiafeng Wang, Email zzshuang2000@126.com; wjfeng2000@126.com

Background: Atopic Dermatitis (AD) is a common continuous inflammation dermatosis requiring efficacious therapeutic intervention. Phellodendri Chinensis Cortex-Cnidii Fructus (PC) herb pair has shown effectiveness and security in traditional Chinese medicine (TCM) clinical applications, yet its pharmacological constituents and mechanisms are not fully elucidated.

Purpose: This study used serum pharmacology, network pharmacology, and validation experiments to examine the impact of PC in the treatment of AD.

Methods: Initially, ultra performance liquid chromatography-mass spectrometry (UPLC-MS) had been applied to elucidate the components of PC that were absorbed. An integrative approach combining network pharmacology and in vivo research (general index observation, skin pathological tissue staining, ELISA, immunohistochemistry, immunofluorescence, and Western blotting) was employed to validate PC's mechanism in action after 2,4-dinitrochlorobenzene (DNCB) was used to create a mouse model of AD.

Results: Fifty-three compounds and 18 serum prototype components were characterized within PC. The therapeutic efficacy of PC in AD was notably manifested in the alleviation of pruritus, improvement of skin histopathology, and reduction of cytokines involving IgE, IL-4, TNF- α and IL-6. Based on molecular docking studies, pharmacodynamic components such as phellodendrine, xanthotoxin, nomilin, and isopimpinellin strongly favored the main targets. Comprehensive investigations integrating serum pharmacology, network pharmacology, and in vivo studies had revealed that PC prevented DNCB-induced AD through adjusting the TLR4/NF- κ B signaling pathway.

Conclusion: The anti-AD effects of PC may be attributed to its modulation of the TLR4/NF- κ B signaling pathway, reduction of NF- κ B expression in the nucleus, downregulation of inflammatory cytokine levels, improvement of skin histopathological manifestations, and reduction of skin pruritus.

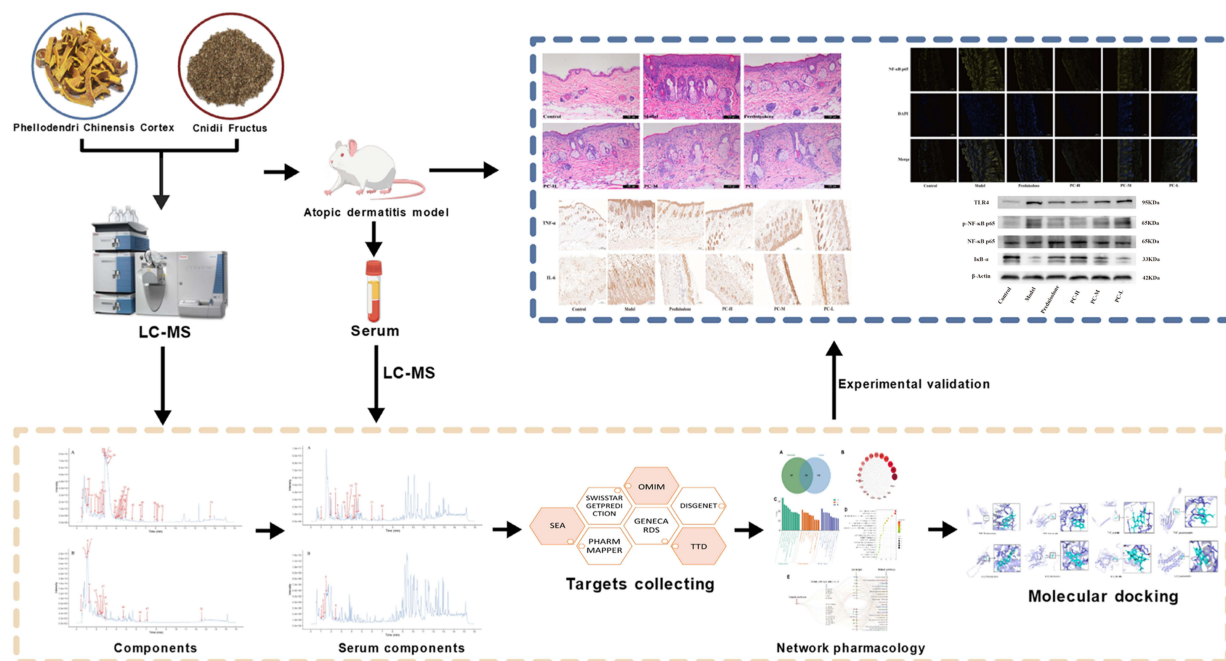
Keywords: Phellodendri Chinensis Cortex, Cnidii Fructus, atopic dermatitis, serum pharmacology, network pharmacology, mechanism

Introduction

Atopic dermatitis (AD), synonymous with atopic eczema, manifests clinically with a spectrum of symptoms, including chronic pruritus and eczematous skin lesions. The etiologic underpinnings of AD are multifaceted, with contemporary medical science attributing its pathogenesis predominantly to genetic predispositions, compromised integumentary barrier function, and aberrations in immune response mechanisms.¹ Around 13% of kids and 5% of mature individuals globally suffer from AD, the most common chronic inflammatory skin condition.² It has been stated that 11% of adolescents under the age of 17 in the US have AD, with an early onset observed in approximately 85% of AD patients



Graphical Abstract



before the age of 5. Moreover, a significant proportion ranging from 20% to 40% of children diagnosed with AD experience a persistent course extending into adulthood.^{3,4} In addition to its chronic and relapsing nature, AD is associated with other allergic disorders, potentially presenting concurrent conditions such as asthma and allergic rhinitis in patients. It has been observed that nearly half of children with AD may progress to develop asthma.⁵ Recent research findings suggest a significant correlation between AD and hypertension, diabetes, heart disease, autoimmune disorders, and mental health conditions. Moreover, the severity of AD is positively associated with the prevalence of these diseases.⁶ AD presents substantial challenges to patients, exerting physiological, psychological, and socio-economic impacts. Current Western pharmaceuticals for the treatment of AD include glucocorticoids, antihistamines, immunosuppressants, and biologic agents, all of which have certain limitations and side effects. For instance, the long-term use of glucocorticoids can lead to resistance and adrenal suppression in target tissues, particularly in individuals with high sensitivity to glucocorticoids. This can result in significant weight gain and other side effects. The side effects of glucocorticoids can affect almost every organ system in the body, causing a range of conditions such as muscle atrophy, hyperglycemia, insulin resistance, hypertension, dysregulation of fat deposition, and osteoporosis.⁷ On the other hand, biologic agents, which have fewer side effects, are often expensive, imposing a financial burden on patients who need ongoing therapy.

Traditional Chinese medicine (TCM) offers notable therapeutic efficacy with comparatively lower side effects and relapse rates in the treatment of skin diseases, providing a perfect choice for AD treatment. Phellodendri Chinensis Cortex-Cnidii Fructus (PC) is a herbal couplet that is a commonly employed therapeutic combination in TCM for the management of AD.

Phellodendri Chinensis Cortex, first documented in the *Shen Nong Ben Cao Jing*,⁸ belongs to the Rutaceae family and is made from the dried bark of *Phellodendron chinense* Schneid.⁹ Because of its ability to clear heat and dry dampness, detoxify, and promote the healing of sores, it has long been used for the treatment of external injuries and conditions characterized by redness, swelling, and ulceration of the skin or mucous membranes.¹⁰ Phellodendri Chinensis Cortex has been shown to alleviate skin inflammation associated with AD by inhibiting the activity of the progranulin (PGRN) gene along with protein, thereby reducing the levels of tumor necrosis factor- α (TNF- α). This reduction in TNF- α

contributed to the amelioration of skin redness, scaling, crusting, and exudate, which are common manifestations of the disease.¹¹ Berberine, a constituent of *Phellodendri Chinensis Cortex*, has been found to inhibit the expression of mucosa-associated lymphoid tissue lymphoma translocation gene 1 (MALT1) and the eukaryotic translation initiation factor 3F (EIF3F). This inhibition led to a decrease in the production of macrophage migration inhibitory factor (MIF) and interleukin-4 (IL-4), which are key mediators of the inflammatory response in AD.¹² The combined use of *Phellodendri Chinensis Cortex* capsules and olopatadine hydrochloride has been demonstrated to significantly reduce skin lesions in rats with acute eczema. The downregulation of interferon- γ (IFN- γ), IL-4, and TNF- α levels, together with the protein and mRNA expression of intercellular adhesion molecule-1 (ICAM-1) and vascular endothelial cell adhesion molecule-1 (VCAM-1), may be the cause of this therapeutic effect.¹³

Cnidii Fructus, also first mentioned in the *Shen Nong Ben Cao Jing*,⁸ is the dried mature fruit of the Apiaceae plant *Cnidium monnieri* (L.) Cuss.⁹ It has the ability to eliminate parasites, disperse wind, dry out moisture, and relieve itching, which are beneficial in treating conditions such as eczema and urticaria. Its therapeutic effects extend to alleviating symptoms like itching caused by inflammation in allergic diseases.¹⁴ The synergistic action of these two herbs is believed to enhance their therapeutic efficacy when used in combination. This traditional herbal pairing exemplifies the holistic and synergistic approach of TCM. A topical powder prepared from *Cnidii Fructus* has been demonstrated to effectively ameliorate skin lesions in a rat model of eczema, repair pathological damage, and reduce the levels of inflammatory cytokines. Restoring the balance within Th1 and Th2 cells may be achieved by promoting the production of IFN- γ and suppressing the release of allergenic mediators like IL-4, IL-18, with IL-33.¹⁵ The active component of *Cnidii Fructus*, known as osthole, has been shown to regulate the generation of tight junction proteins in AD mice models' skin through phosphatidylinositol 3-kinases (PI3K)/protein kinase B (AKT) pathway. This regulation significantly increased the mRNA production of zonula occludens (ZO)-1, ZO-2, ZO-3, ZO-4, claudin (CLDN)-1, CLDN-6, and CLDN-23 while decreasing the mRNA expression of junctional adhesion molecule (JAM)-1, JAM-2, CLDN-5, along with CLDN-15, which contributes to the reduction of inflammatory responses and the alleviation of chronic scratching behavior.¹⁶ Furthermore, osthole significantly inhibited the overproliferation of mast cells in eczematous mice and promoted their apoptosis, possibly through the downregulation of signal transducer and activator of transcription 5 (STAT5) gene and protein development.¹⁷

The synergistic action of these two herbs is believed to enhance their therapeutic efficacy when used in combination. This traditional herbal pairing exemplifies the holistic and synergistic approach of TCM. A clinical study has found that the use of a formula composed of PC in conjunction with pevisone cream significantly reduces the severity of itching, the area of skin lesions, and the symptom score of skin lesion morphology in patients with eczema, with a higher efficacy rate compared to the use of pevisone cream alone.¹⁸ After treatment with the Huangdi formula, which is composed of PC, a noticeable decrease in Immunoglobulin E (IgE) levels and a decline in the amount of CD8⁺ cells and a rise in the ratio of CD4⁺ cells were observed in children with eczema's peripheral blood. This suggests that Huangdi Tang may participate in the immunoregulation of children with eczema by modulating the balance of CD4⁺/CD8⁺ cells and/or downregulating the expression of IgE, achieving therapeutic goals, with a lower recurrence rate compared to the hydrocortisone butyrate group.¹⁹ In a study observing the efficacy of 180 patients with acute eczema, the findings indicated no discernible disparity in therapeutic effects amongst the groups receiving pevisone and PC ointment, with better outcomes than the group treated with Bing Huang Fu Le ointment, and no drug-related adverse reactions were observed.²⁰ Despite the promising clinical efficacy of PC in treating eczema and other skin diseases, modern research on its pharmacological components and therapeutic mechanisms remains limited. Specifically, the mechanisms underlying its effects on AD are poorly understood. To address this gap, we hypothesize that PC may exert therapeutic effects on AD by modulating specific signaling pathways. This study aims to systematically evaluate the therapeutic potential of PC in an AD mouse model for the first time and elucidate its potential active constituents and underlying mechanisms. By doing so, we aim to uncover novel therapeutic targets and provide a comprehensive mechanistic understanding of PC's effects on AD, thereby contributing to the limited body of research in this area.

The bioactive constituents of herbal medicine are associated with the materials and components that enter the circulation and undergo metabolism following oral administration. Currently, serum pharmacology has emerged as a practical approach for investigating the active components of herbal medicine.²¹ Network pharmacology, which

integrates theories from systems biology, bioinformatics, and computer science, provides advanced approaches for elucidating the comprehensive mechanisms underlying the therapeutic effects of TCM.²² Through a series of assays, we assessed PC's effects on a mouse model of AD produced by 2,4-dinitrochlorobenzene (DNCB). Subsequently, depending on ultra performance liquid chromatography-mass spectrometry (UPLC-MS), we investigated potential effective constituents and therapeutic mechanisms through combining serum pharmacology coupled with network pharmacology. Furthermore, the connections amongst the active ingredients of PC and crucial targets linked to AD were confirmed using molecular docking. Additionally, in vivo experiments were conducted to substantiate the hypothesis that toll-like receptor 4 (TLR4)/Nuclear factor- κ B (NF- κ B) signaling pathway is implicated in the effects of PC on AD.

Materials and Methods

Materials

PC's elements include two Chinese herbal medicines, including 60g of *Phellodendri Chinensis Cortex* (*Huangbo*, Lot No. B22123101-01) and 30g of *Cnidii Fructus* (*Shechuangzi*, Lot No. 20200601). Every TCM material was provided from Shandong Jianlian Shengjia Traditional Chinese Medicine Store (Jinan, China). The quality control tests of the two TCM herbs were conducted according to the methods specified in *Pharmacopoeia of the People's Republic of China 2020*, and the test results complied with the established standards (Table S1, Figure S1).

Animals

Six-week-old male BALB/c mice, SPF grade, weighing 18–22 g, were acquired by Beijing Vital River Laboratory Animal Technology Co., Ltd. (Beijing, China), with a certificate number SCXK (Jing) 2021–0006. The experimental animals were raised in SPF-grade animal facility of the Experimental Animal Center at Shandong University of Traditional Chinese Medicine under controlled conditions (22–24 °C, 40%–60% humidity, 12 h light/dark cycle), with unlimited access to food and water. The research procedure was authorized by the Ethics Review Committee for the Welfare of Experimental Animals at Shandong University of Traditional Chinese Medicine and was conducted in compliance with the Animal Experiment Ethics Code 2022–7 (approval number: SDUTCM20230228001).

Preparation of Drug

A precisely measured 60g of *Phellodendri Chinensis Cortex* and 30 g of *Cnidii Fructus* were subjected to a maceration process with a 10-fold volume of distilled water for 30 min, followed by 1 h extraction. The resultant decoction was immediately filtered through a four-layer gauze. The residue underwent a secondary extraction with an 8-fold volume of distilled water for 1 hour and was similarly filtered. The combined filtrates were concentrated to achieve a 2 g/mL concentration equivalent to the raw herbal material.

Prednisolone is a common immunologic drug that is used clinically for the treatment of pruritic skin diseases,⁷ and is administered orally in the same manner as PC. Prednisolone (H41020283, Tianfang Pharmaceutical Co., Ltd., Zhumadian, China) was solubilized in distilled water to formulate a solution at a concentration of 1 mg/mL.

Construction of Mouse AD Model

Seventy-two mice were divided into 6 groups: control group (n=12), model group (n=12), prednisolone group (n=12), PC-H group (n=12), PC-M group (n=12), and PC-L group (n=12). With the exception of the control group, an AD model was induced in the other groups of mice using a modified method based on previously published literature.²³ After a one-week acclimation period, on the day prior to the experiment (Day 0), the mice's dorsal fur was depilated employing depilatory cream. On Day 1 and Day 4, excluding the control group, 150 μ L of 1% DNCB was administered uniformly to the mice's depilated dorsal region. From Day 7 to Day 28, every 48h, excluding the blank control group, an application of 100 μ L of 0.5% DNCB was administered to the depilated dorsal area of each mouse. The control group received an equal volume of acetone-olive oil vehicle on their depilated dorsal area with matching timing and dosage as other groups. The mice's backs showed blood crusts, scales, dark erythema, hyperkeratosis, and hypertrophy of the skin spinous layer following the final modeling session, suggesting that the model was effective.²⁴ Converted from "Equivalent dose ratios

for human and animal body surface area conversion”,²³ the medium dose of PC for animals was calculated to be 2.86 mg/g/d, which is equivalent to the clinical dosage. To assess the impact of PC on AD mice, different doses of PC (1.43, 2.86, 5.72 mg/g/d) were orally administered to the low, medium, and high-dose groups from day 10 to day 29 of the experiment, respectively. The prednisolone group received an oral solution of prednisolone at a dosage of 0.01 mg/g/d. The blank control group and model group mice were gavage-fed an equal volume of distilled water.

Observation Indicators

Observations on the General Condition and Scratching Behaviour of Mice

The general condition of mice was monitored on a daily basis. Following the final modeling procedure, the frequency of dorsal skin scratching in mice was quantified over a 10-min duration.

Scoring of Dermal Inflammation Severity

Mice dorsal skin inflammation was evaluated through a scoring system based on four symptoms: erythema/hemorrhage, dryness/dandruff, edema, and desquamation/ulceration.²⁵ The severity of each symptom was graded as follows: 0 (none), 1 (mild), 2 (moderate), and 3 (severe). Detailed criteria for scoring can be found in [Table S2](#).

Sample Collection

Before euthanasia, blood collection was performed via ocular venipuncture following the final administration of treatment. The collected blood was left at room temperature for 30 min before being centrifuged at 4 °C and 3000 rpm for 15 min to separate the serum, which was subsequently stored at -80°C. Segments of dorsal mouse skin were harvested, with a portion fixed in 4% paraformaldehyde and the remainder stored at -80°C for future use.

Identification of Chemical Constituents of PC and Serum Absorbed Prototype

Constituents by UPLC-MS

Preparation of PC Sample Solution

The PC aqueous is vortexed for 30s and then centrifuged at 4 °C at 12000 rpm for 15 min. Subsequently, 300 µL of the supernatant is transferred into an EP tube, to which a mixture of methanol and water in a proportion of 4:1 (with an internal standard concentration of 10 µg/mL) is added (1000 µL). After additional vortexing for 30s, the mixture is ultrasonicated in an ice-water bath for 5 min, followed by incubation at -40°C for one hour. The solution is then subjected to another round of centrifugation at 4°C at a speed of 12000 rpm for 15 min. Finally, the supernatant undergoes filtration via 0.22 µm-pore microporous membrane to produce the sample solution that is prepared for analysis.

Preparation of Serum Samples

Serum samples are prepared by acidifying with 2 mol/L HCl, followed by sequential vortexing and standing for 15 min, repeated quadruple. Subsequently, 1.6 mL acetonitrile is integrated, the mixture is vortexed for 5 minutes, and centrifuged at 12,000 rpm for 5 minutes to precipitate proteins. 1800 µL supernatant is aspirated and evaporated under nitrogen. The residue is then redissolved in 150 µL of 80% methanol with an internal standard at 10 µg/mL, vortexed, centrifuged, and the supernatant is collected for analytical readout.

UPLC-MS Analysis Conditions

The detection of PC sample solution and serum samples was performed using UPLC-MS (Thermo Fisher Scientific, MA, USA). Chromatographic separation was achieved using an ACQUITY UPLC BEH-C18 column (2.1×100mm, 1.7µm, Waters, MA, USA) with a column temperature of 55°C. The mobile phase consisted of 0.1% formic acid in water (Solvent A) and 0.1% formic acid in acetonitrile (Solvent B). Gradient elution was performed as follows: from 0 to 11 minutes, the solvent composition was increased from 15% B to 75% B; from 11 to 12 minutes, it was increased further to 98% B; then held at 98% B from 12 to 14 minutes. After that, the composition was rapidly decreased back to 15% B over 0.1 minutes (from 14 to 14.1 minutes) and finally maintained at 15% B from 14.1 to 16 minutes. The flow rate

was set at 0.5 mL/min. Sheath gas flow rate: 35 Arb, Aux gas flow rate: 15 Arb, Ion Transfer Tube Temp: 350°C, Auxillary gas Temp: 350°C, Scan range: 100–1500 *m/z*, Collision energy: 16/32/48, Spray Voltage: 4 kV (positive) and –3.8 kV (negative). Data processing was conducted utilizing the XCMS software, and target compounds were determined using the secondary database of TCM MS/MS Library.

Network Pharmacology Study and Molecular Docking

The chemical substances identified in mouse serum may serve as effective components of PC. Extract their corresponding targets from SEA (<https://sea.bkslab.org/>), SwissTargetPrediction (<http://www.swisstargetprediction.ch/>), and PharmMapper (<https://lilab-ecust.cn/pharmmapper/index.html>). Subsequently, a systematic screening of AD-related targets was conducted employing OMIM (<https://omim.org/>), GENECARDS (<https://www.genecards.org/>), TTD (<https://db.idrblab.net/ttd/>), and DisGeNET (<https://www.disgenet.org/>). Target names were standardized through UniProt (<https://www.uniprot.org/>). The intersection of targets was delineated employing a Venn diagram constructed via Weishengxin (<https://www.bioinformatics.com.cn/>) to identify potential targets for PC treatment of AD. These intersection targets were subsequently subjected to a protein–protein interaction (PPI) network analysis within String (<https://string-db.org/>). The PPI network file was topologically analyzed by Cytoscape 3.9.1 software. Furthermore, major targets implicated in PC-mediated AD treatment were subjected to Gene Ontology (GO) enrichment analysis using DAVID (<https://david.ncifcr.gov/>), encompassing biological process (BP), cell component (CC) and molecular function (MF) aspects, along with Kyoto Encyclopedia of Genes and Genomes (KEGG) pathway enrichment analysis.

Three-dimensional structures of the top six protein receptor genes with the highest degree values were acquired from the PDB (<http://www.rcsb.org/>). Subsequently, two-dimensional structures of the primary PC chemicals, confirmed as ligands through UPLC-MS, were extracted from the PubChem (<https://pubchem.ncbi.nlm.nih.gov/>). The Chem3D software suite was then employed to transform these structures into three-dimensional representations. Binding affinity between receptors and ligands was determined through AutoDock software. Lastly, PyMOL was applied to visualize the results.

Experimental Verification

H&E Staining

The skin tissues of mice were fixed in 4% paraformaldehyde solution for 24 h, followed by dehydration and paraffin embedding. Subsequently, sections with a thickness of 3 μm were prepared. These sections were then stained using Hematoxylin and Eosin (Servicebio, Wuhan, China) following the manufacturer's protocol. Histopathological changes were observed under a light microscope (Leica, Wetzlar, Germany).

Elisa

The levels of IgE, IL-4, TNF- α and IL-6 in serum were quantified following the protocols provided with the IgE assay kit, IL-4 assay kit, TNF- α assay kit and IL-6 assay kit, both obtained from Shanghai Enzyme-Linked Biotechnology Co., Ltd. (Shanghai, China). Absorbance value at 450 nm was measured using microplate reader (BioTek, VT, USA).

Immunohistochemistry (IHC)

Paraffin-embedded sections were deparaffinized, rinsed, and subjected to antigen retrieval in citrate buffer (pH 6.0) (Akoya Biosciences, MA, USA) using microwave. After cooling, slides were washed in TBST and incubated with 3% H₂O₂ to block endogenous peroxidase. Following a 30-min incubation with goat serum (Boster, CA, USA), sections were probed with antibodies against TNF- α (ABCAM, Cambridge, UK) and IL-6 (ABCAM) for 1 h. The DAB substrate kit was utilized for visualization, and slides were analyzed using SlideViewer 2.6.0 (3DHISTECH, Budapest, Hungary).

Immunofluorescence (IF)

Paraffin-embedded sections were deparaffinized, rinsed, and subjected to antigen retrieval in citrate buffer (pH 6.0) (Akoya Biosciences) using microwave. After cooling, slides were washed in TBST and incubated with 3% H₂O₂ to block endogenous peroxidase. Following a 30-min incubation with goat serum (Booster), sections were probed with NF- κB p65

Polyclonal antibody (10745-1-AP, Proteintech, CHI, USA) for 1 h. Subsequent incubation with Opal Polymer HRP Ms +Rb (Akoya Biosciences) for 10 min and Opal 520 (Akoya Biosciences) for 5 min facilitated signal enhancement. Nuclear counterstaining was performed with DAPI (Akoya Biosciences). Slides were scanned using a slide scanner and analyzed with SlideViewer 2.6.0 (3DHISTECH).

Western Blot

The total proteins were separated using SDS-PAGE and subsequently transferred onto PVDF membranes (Millipore, MA, USA). After blocking with 5% non-fat dry milk in TBST for 1.5 h, the membranes were incubated overnight at 4°C with anti-TLR4 antibody (sc-293072, Santa Cruz Biotechnology, CA, USA), anti-IkB- α antibody (10268-1-AP, Proteintech), anti-NF- κ B p65 antibody (10745-1-AP, Proteintech), and anti-p-NF- κ B p65 antibody (CPA1998, Cohesion, London, UK). Following three washes with TBST, the membranes were incubated with HRP-conjugated goat anti-rabbit IgG (ABclonal, Boston, USA) and goat anti-mouse IgG (ABclonal) for 1 h at room temperature. Protein detection was performed using an enhanced chemiluminescence kit and quantified utilizing multicolor fluorescence imaging system (GE, CHI, USA).

Statistical Analysis

Data analysis was performed using SPSS 25.0, and graphical representations were created with GraphPad Prism 9.5. Data were presented as mean \pm SD. Significant difference was established at $P < 0.05$.

Result

PC Improved Symptoms in AD Mice

To validate the protective effects of PC on AD, AD model was established. Mice in the control group exhibited normal mental states without agitation or abnormal behavior. In contrast, the model group displayed significant agitation and intense resistance when handled after modeling. No discernible changes were seen at control mice's dorsal surface following application of the vehicle. Conversely, the model group initially exhibited acute inflammatory reactions, such as edema, after the initial DNCB application. With subsequent applications, chronic changes including erythema, ulceration, and crust formation occurred along with dryness and desquamation, ultimately leading to gradual formation of yellow-brown crusts on the skin surface. Contrasted with the model group, mice given varying doses of PC and prednisolone demonstrated progressive alleviation of erythema, ulceration, and crusting, indicating a significant inhibitory effect of PC against DNCB-induced AD. Notably, high-dose PC and prednisolone had similar levels of effectiveness and superior to the medium and low doses (Figure 1A).

As seen in Figure 1B, mice in the model group had a slightly lower body weight during the treatment period than mice in the control group; however, there was no statistically significant difference ($P > 0.05$). Figure 1C showed that scratching was far more common in the model group than control group ($P < 0.01$), and this frequency was markedly reduced in the PC-H, PC-M, and PC-L groups, as well as the prednisolone group ($P < 0.01$). As illustrated in Figure 1D, there was a significant elevation in skin lesion scores for the model group contrasted with the control group ($P < 0.01$). Skin lesion ratings were significantly reduced after PC therapy ($P < 0.01$ or $P < 0.05$).

Identification of Compounds and Absorbable Prototypes in PC

53 Compounds Within the PC Were Identified Using UPLC-MS

PC extract was characterized by the presence of alkaloids, coumarins, limonoids, flavonoids, chromones, and phenolic acids. A total of 53 constituents were identified through UPLC-MS analysis. Eleven alkaloids were defined from PC, including protoberberine, tetrahydroprotoberberine, benzyloquinoline, aporphine alkaloids, and others. Among the identified alkaloids were berberine, berberrubine, palmatine, dehydroevodiamine, skimmianine, phellodendrine, magnoflorine, jatrorrhizine, γ -fagarine, N-methylflindersine, and canthin-6-one. A total of 14 coumarins, including osthole, bergapten, bergaptol, imperatorin, isoimperatorin, isopimpinellin, 7-Demethylsuberosin, xanthotoxin, xanthotoxol, auraptenol, fraxetin, and 8-Hydroxybergapte, were identified from the aqueous extract of PC. These compounds were categorized into simple

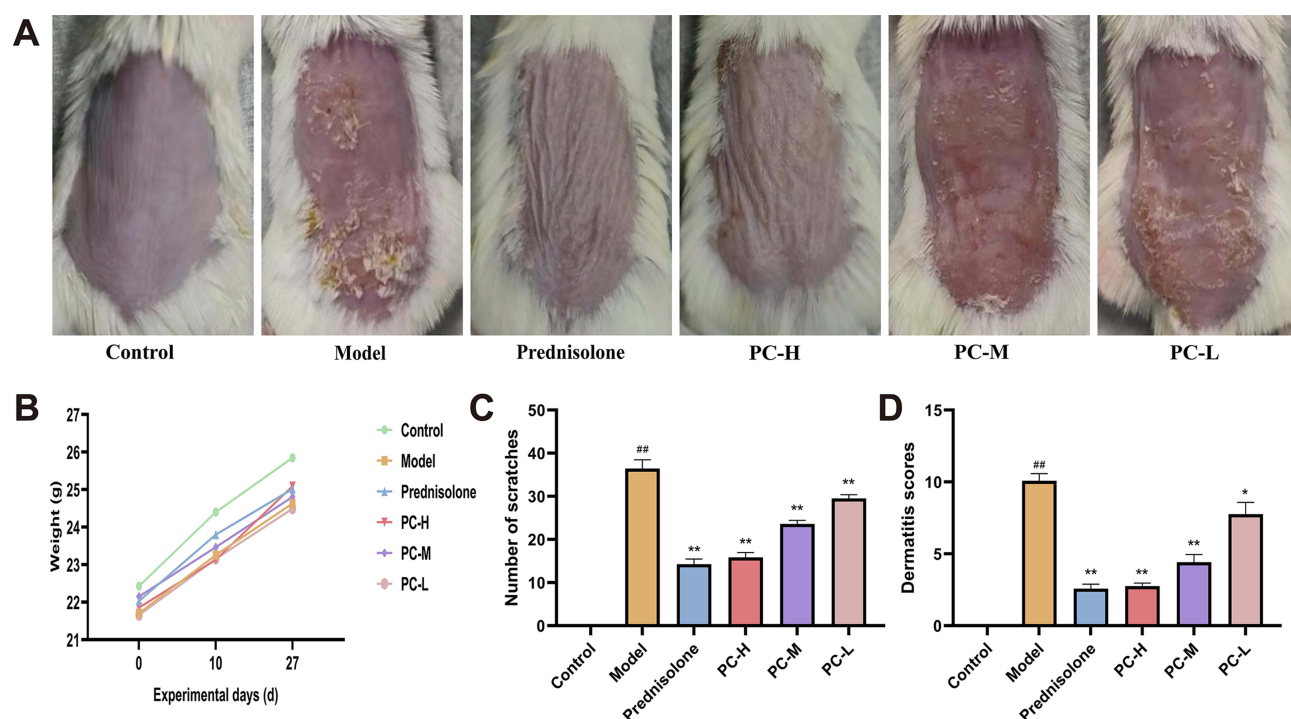


Figure 1 Effects of PC on the AD model in vivo **(A)** Dermatological manifestations of skin lesions in mice across all experimental groups. **(B)** Body weight changes in mice over the course of the study. **(C and D)** Bar graphs of the number of scratches and dermatitis scores in each group. ^{###} $P < 0.01$ vs control group. ^{*} $P < 0.05$, ^{**} $P < 0.01$ vs model group.

coumarins and furanocoumarins. In the PC extract, 4 limonoid compounds were identified, comprising rutaevin, obacunone, limonin, and nomilin. Six flavonoids were detected, namely kaempferol, quercetin, rutin, hesperidin, hyperoside, and icariin. The PC aqueous extract also contained 3 chromones, including 5-O-methylvisammioside, cimifugin, and noreugenin. Furthermore, 5 phenolic acids were detected, which include quinic acid, ferulic acid, chlorogenic acid, caffeic acid, and isochlorogenic acid B. Beyond the aforementioned compounds, the PC aqueous extract was also found to contain sterols, fatty acids, and other classes of compounds. These included stigmasterol, linoleic acid, oleic acid, 4-hydroxystyrene, styrene, perillene, coniferin, anisic aldehyde, 5-hydroxymethylfurfural, and cassiastearoptene. The total ion chromatogram is presented in [Figure 2](#) with detailed mass spectrometry data provided in [Table 1](#).

18 Prototype Components Absorbed Into the Blood Were Identified by UPLC-MS

By comparing the chromatogram of the drug-containing serum with that of the blank serum ([Figure 3](#)) and the PC aqueous extract, a total of 18 prototype components absorbed into the blood were identified, including alkaloids, coumarins, limonoids, flavonoids, and phenolic acids. Specifically, these components are chlorogenic acid, quinic acid, phellodendrine, 4-hydroxystyrene, rutin, kaempferol, icariin, nomilin, bergaptol, 8-hydroxybergapten, xanthotoxol, auraptanol, canthin-6-one, xanthotoxin, skimmianine, rutaevin, isopimpinellin, and N-methylflindersine. Among them, phellodendrine, skimmianine, rutaevin, nomilin, canthin-6-one, and N-methylflindersine were derived from *Phellodendri Chinensis Cortex*, while bergaptol, xanthotoxin, 8-hydroxybergapten, xanthotoxol, auraptanol, and isopimpinellin were derived from *Cnidii Fructus*. Detailed information can be found in [Table 2](#). The obtained serum samples were analyzed using UPLC-MS. The total ion chromatograms of the mouse serum containing PC drug is presented in [Figure 4](#). The structures of the 18 serum prototype components are shown in [Figure 5](#).

Network Pharmacology

The Potential Therapeutic Targets of PC for AD

By utilizing the SEA, SwissTargetPrediction, and PharmMapper databases, we identified 18 prototype components (chlorogenic acid, quinic acid, phellodendrine, 4-hydroxystyrene, rutin, kaempferol, icariin, nomilin, bergaptol,

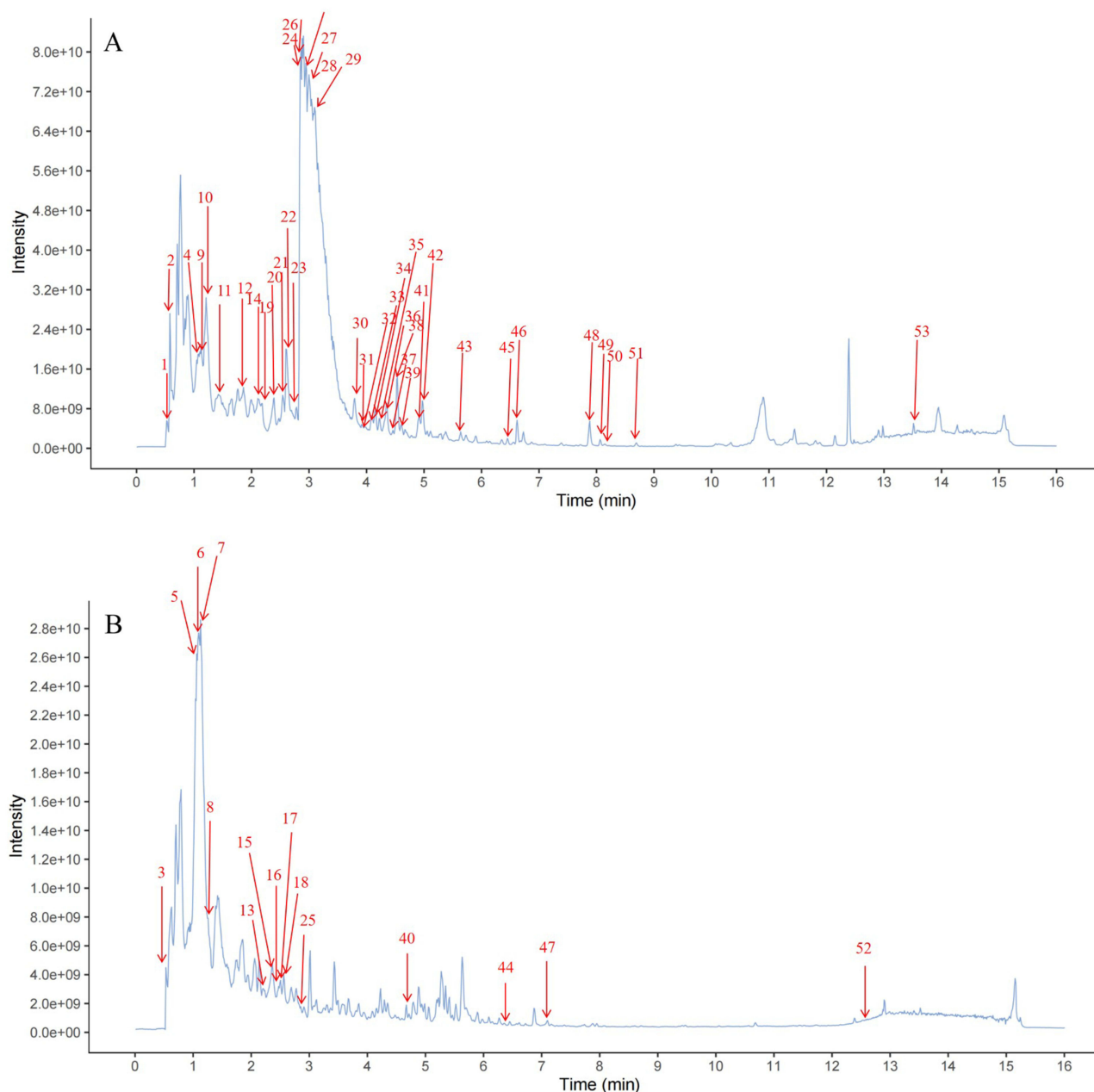


Figure 2 Total ion chromatograms of PC aqueous extract. **(A)** Positive ion mode. **(B)** Negative ion mode.

8-hydroxybergapten, xanthoxol, auraptanol, canthin-6-one, xanthotoxin, skimmianine, rutaevin, isopimpinellin, and N-methylflindersine) that were absorbed into the blood. After that, deduplication process was performed on these components' targets, resulting in a total of 965 target points. We obtained a collection of AD-related targets by employing "atopic dermatitis" as the keyword in OMIM, TTD, DisGeNET, and GENECARDS databases which yielded a total of 1834 targets after deduplication. By comparing the targets related to PC's absorbed components with AD-related targets, a set of intersection consisting of 298 potential therapeutic targets for PC in treating AD was identified as shown in Figure 6A. The information regarding these potential target proteins was imported into String platform where homo sapiens attribute was chosen and minimum required interaction score placed at 0.700 to obtain TSV format file containing protein interaction relationships. After calculating the median degree value, 20 targets were deemed critical

Table 1 Phytochemical Constituents Discovered in PC Aqueous Extract

No.	Name	Formula	m/z	t _R	ppm	ms2Adduct	MS2
1	Fraxetin	C ₁₀ H ₈ O ₅	209.0450	26.5009	3.0359	[M+H] ⁺	209.0438;179.0340;210.0491;138.0310;103.0176
2	Styrene	C ₈ H ₈	105.0698	27.3382	1.8827	[M+H] ⁺	105.0703;91.0541;106.0786;79.0544;103.0540
3	Caffeic acid	C ₉ H ₈ O ₄	179.0351	45.7197	0.6032	[M-H] ⁻	135.0460;179.0355;164.0116;136.0160;59.0141
4	Chlorogenic acid	C ₁₆ H ₁₈ O ₉	372.1260	67.9975	0.0901	[M+H] ⁺	86.0960;177.0539;373.1812;192.1014;193.1060
5	Quinic acid	C ₇ H ₁₂ O ₆	191.0558	68.8179	4.1480	[M-H] ⁻	191.0558;85.0295;111.0089;87.0084;93.0341
6	Phellodendrine	C ₂₀ H ₂₄ NO ₄ ⁺	340.1556	78.9641	1.8814	[M-2H] ⁻	340.1583;78.9589;310.1076;325.1292;152.9963
7	4-Hydroxystyrene	C ₈ H ₈ O	119.0501	83.8328	1.2404	[M-H] ⁻	119.0509;59.0141;121.0295;120.0549;75.0086
8	Rutin	C ₂₇ H ₃₀ O ₁₆	609.1445	85.1943	2.4104	[M-H] ⁻	609.1378;300.0267;301.0339;271.0232;255.0319
9	Quercetin	C ₁₅ H ₁₀ O ₇	303.0505	85.2189	1.6341	[M+H] ⁺	303.0477;86.0961;229.0482;144.1023;257.0456
10	Ferulic acid	C ₁₀ H ₁₀ O ₄	195.0655	85.6978	2.7645	[M+H] ⁺	177.0539;145.0287;178.0595;146.0320;107.0488
11	Hyperoside	C ₂₁ H ₂₀ O ₁₂	463.1035	97.3160	1.0596	[M+H] ⁺	303.0479;86.0962;120.0809;85.0282;72.0810
12	Kaempferol	C ₁₅ H ₁₀ O ₆	287.0560	117.4115	3.3511	[M+H] ⁺	287.0572;177.0542;227.1081;255.1026;195.0804
13	Coniferin	C ₁₆ H ₂₂ O ₈	341.1241	122.4240	3.1897	[M-H] ⁻	341.1248;305.0672;59.0138;165.0930;342.1320
14	5-Hydroxymethylfurfural	C ₆ H ₆ O ₃	127.0391	128.5630	1.0979	[M+H] ⁺	127.0399;128.0711;114.9716;109.1009;83.0497
15	Isochlorogenic acid B	C ₂₅ H ₂₄ O ₁₂	515.1210	146.0120	3.9474	[M-H] ⁻	353.0890;173.0464;179.0355;191.0563;135.0459
16	Icariin	C ₃₃ H ₄₀ O ₁₅	721.2357	146.9300	0.9041	[M+FA] ⁻	721.2264;191.0572;96.9601;93.0346;173.0445
17	Nomilin	C ₂₈ H ₃₄ O ₉	513.2118	147.9715	1.6229	[M-H] ⁻	513.2050;173.0463;96.9598;467.2457;351.0717
18	Hesperidin	C ₂₈ H ₃₄ O ₁₅	609.1835	152.4690	0.7816	[M-H] ⁻	301.0712;609.1729;286.0470;164.0116;242.0575
19	Berberrubine	C ₁₉ H ₁₅ NO ₄ ⁺	322.1078	154.2750	2.5419	[M+H] ⁺	322.1057;307.0836;279.0875;323.1087;308.0877
20	Jatrorrhizine	C ₂₀ H ₂₀ NO ₄ ⁺	338.1392	157.7765	0.5013	[M] ⁺	338.1386;323.1151;322.1063;294.1103;308.0949
21	Cassiastearoptene	C ₁₀ H ₁₀ O ₂	163.0754	160.0150	2.5847	[M+H] ⁺	163.0382;131.0485;164.0480;139.9826;162.0309
22	Bergaptol	C ₁₁ H ₆ O ₄	203.0339	160.9150	0.7238	[M+H] ⁺	203.0329;204.0370;175.0379;147.0440;159.0444
23	Dehydroevodiamine	C ₁₉ H ₁₅ N ₃ O	302.1287	164.2620	1.0119	[M+H] ⁺	302.1311;287.1040;286.0959;303.1305;247.9755
24	7-Demethylsuberosin	C ₁₄ H ₁₄ O ₃	231.1016	165.1630	2.7421	[M+H] ⁺	190.0565;232.1044;189.0539;191.0601;132.0523
25	Noreugenin	C ₁₀ H ₈ O ₄	191.0350	171.3590	0.1913	[M-H] ⁻	191.0342;147.0452;149.0239;85.0296;192.0398
26	Palmatine	C ₂₁ H ₂₂ NO ₄ ⁺	352.1529	173.2070	2.9825	[M] ⁺	352.1548;336.1240;337.1330;308.1269;322.1063
27	Anisic aldehyde	C ₈ H ₈ O ₂	137.0598	196.5880	1.6117	[M+H] ⁺	137.0605;95.0849;81.0702;138.0907;122.0368
28	8-Hydroxybergapten	C ₁₂ H ₈ O ₅	233.0447	199.5045	3.1485	[M+H] ⁺	233.0454;218.0212;173.0229;234.0480;232.1000
29	γ-Fagarine	C ₁₃ H ₁₁ NO ₃	246.0764	202.7250	1.4604	[M+H] ⁺	246.0744;231.0506;247.0759;232.0606;187.0756
30	Berberine	C ₂₀ H ₁₈ NO ₄ ⁺	336.1236	223.8080	1.7850	[M+H] ⁺	336.1241;321.1018;320.0886;292.0975;306.0783
31	Xanthotoxol	C ₁₁ H ₆ O ₄	203.0341	227.9810	0.5217	[M+H] ⁺	203.0330;147.0440;175.0379;131.0487;204.0369
32	Auraptanol	C ₁₅ H ₁₆ O ₄	243.1021	228.0500	0.3246	[M-H ₂ O+H] ⁺	189.0536;245.0810;131.0484;147.0437;203.1058
33	Murracarpin	C ₁₆ H ₁₈ O ₅	291.1235	247.4330	1.8404	[M+H] ⁺	221.0715;293.2100;275.1983;220.0689;81.0694
34	5-O-Methylvisammioside	C ₂₂ H ₂₈ O ₁₀	453.1771	248.7370	2.3590	[M+H] ⁺	273.1110;219.0648;291.1234;255.1027;231.0633
35	Canthin-6-one	C ₁₄ H ₈ N ₂ O	221.0709	252.5700	0.3195	[M+H] ⁺	221.0716;222.0734;223.0804;161.1331;203.1063
36	Xanthotoxin	C ₁₂ H ₈ O ₄	217.0496	258.3890	2.9081	[M+H] ⁺	217.0505;202.0258;218.0523;189.0538;185.0244
37	Perillene	C ₁₀ H ₁₄ O	151.1118	258.5840	1.5161	[M+H] ⁺	151.1124;133.1007;107.0849;109.1004;105.0703
38	Skimmianine	C ₁₄ H ₁₃ NO ₄	260.0917	266.4350	0.9656	[M+H] ⁺	202.0914;244.1340;262.0971;229.0642;190.0591
39	Imperatorin	C ₁₆ H ₁₄ O ₄	271.0970	274.0010	0.0203	[M+H] ⁺	203.0331;69.0697;271.0956;147.0439;175.0378
40	Columbianetin	C ₁₄ H ₁₄ O ₄	245.0814	286.6390	2.3890	[M-H] ⁻	245.0832;190.0268;246.0867;175.0398;204.0424
41	Rutaevin	C ₂₆ H ₃₀ O ₉	487.1980	287.3550	0.0558	[M+H] ⁺	337.1254;489.2092;336.1233;322.1056;321.1019
42	Bergapten	C ₁₂ H ₈ O ₄	217.0496	293.2570	1.7374	[M+H] ⁺	217.0506;202.0254;218.0523;189.0190;161.0224
43	Isopimpinellin	C ₁₃ H ₁₀ O ₅	247.0605	335.7625	2.1904	[M+H] ⁺	247.0595;217.0120;232.0340;189.0535;248.0652
44	Obaculactone	C ₂₆ H ₃₀ O ₈	515.1914	381.4850	1.1152	[M+FA] ⁻	469.1863;515.3332;187.0984;191.0563;125.0970
45	N-methylfindersine	C ₁₅ H ₁₅ NO ₂	242.1177	401.8600	1.3471	[M+H] ⁺	188.0708;244.1301;190.0592;189.0538;202.0604
46	Obacunone	C ₂₆ H ₃₀ O ₇	455.2073	413.7145	0.7415	[M+H] ⁺	455.2128;189.0570;81.0703;161.0596;109.1023
47	Isoimperatorin	C ₁₆ H ₁₄ O ₄	269.0816	426.8850	1.6689	[M-H] ⁻	269.0834;62.9643;214.0287;270.0830;201.0176
48	Magnoflorine	C ₂₀ H ₂₄ NO ₄ ⁺	342.1704	462.4075	1.2946	[M] ⁺	192.1021;342.1684;297.1123;265.0873;58.0649
49	Cimifugin	C ₁₆ H ₁₈ O ₆	307.1183	496.7335	0.8303	[M+H] ⁺	307.1168;177.0543;206.0563;289.1771;223.0584
50	Osthole	C ₁₅ H ₁₆ O ₃	245.1176	503.4485	1.6710	[M+H] ⁺	189.0541;131.0488;245.1179;159.0444;161.0600
51	Linoleic acid	C ₁₈ H ₃₂ O ₂	281.2479	523.1480	0.3532	[M+H] ⁺	81.0701;95.0857;69.0700;83.0853;71.0854
52	Oleic acid	C ₁₈ H ₃₄ O ₂	281.2479	750.8340	0.4128	[M-H] ⁻	281.2462;106.0414;282.2512;171.0657;65.0142
53	Stigmasterol	C ₂₉ H ₄₈ O	395.3637	812.1580	3.3918	[M+H] ⁺	395.3646;81.0694;109.1009;95.0859;97.1012

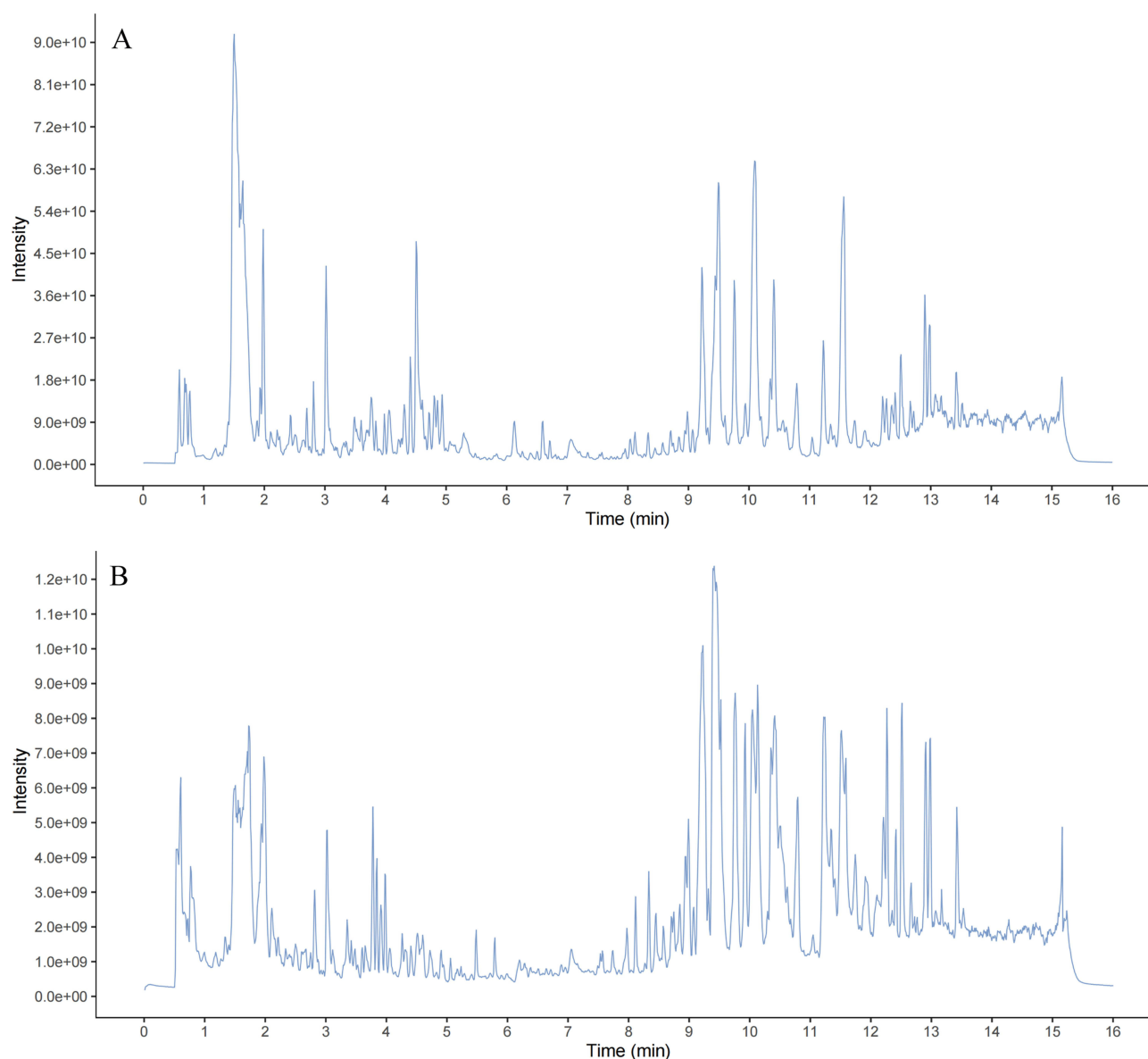


Figure 3 Total ion chromatograms of blank control mice serum. **(A)** Positive ion mode. **(B)** Negative ion mode.

since their degree values were higher than the median (Figure 6B). The top 10 detailed degree, Betweenness Centrality, and Closeness Centrality values were presented in Table 3.

Functional Enrichment Analysis

A total of 298 important targets were subjected to GO study using the DAVID. We chose 754 entries for BP, 83 entries for CC, and 177 entries for MF based on $P < 0.05$. Figure 6C presents the top 10 enriched BP, CC, and MF analysis results in terms of proportion. From the figure, it can be inferred that BP is predominantly enriched in inflammatory response, response to xenobiotic stimulus, response to lipopolysaccharide, negative regulation of apoptotic process, and positive regulation of ERK1 and ERK2 cascade among others. For CC enrichment is mainly observed in plasma membrane, extracellular space, cytosol, integral component of plasma membrane, and cytoplasm. The MF enrichment focuses on enzyme binding, identical protein binding, protein tyrosine kinase activity, endopeptidase activity, and protein homodimerization activity.

Table 2 Prototype Components Identified in PC-Treated Mice Serum

No.	Name	Formula	m/z	t _R	ms2Adduct
1	Chlorogenic acid	C ₁₆ H ₁₈ O ₉	372.1260	67.996	[M+H] ⁺
2	Quinic acid	C ₇ H ₁₂ O ₆	191.0558	68.818	[M-H] ⁻
3	Phellodendrine	C ₂₀ H ₂₄ NO ₄ ⁺	340.1556	78.964	[M-2H] ⁻
4	4-Hydroxystyrene	C ₈ H ₈ O	119.0501	83.833	[M-H] ⁻
5	Rutin	C ₂₇ H ₃₀ O ₁₆	609.1445	85.194	[M-H] ⁻
6	Kaempferol	C ₁₅ H ₁₀ O ₆	287.0560	117.412	[M+H] ⁺
7	Icariin	C ₃₃ H ₄₀ O ₁₅	721.2357	146.930	[M+FA] ⁺
8	Nomilin	C ₂₈ H ₃₄ O ₉	513.2118	147.972	[M-H] ⁻
9	Bergaptol	C ₁₁ H ₆ O ₄	203.0339	160.915	[M+H] ⁺
10	8-Hydroxybergapten	C ₁₂ H ₆ O ₅	233.0447	199.505	[M+H] ⁺
11	Xanthotoxol	C ₁₁ H ₆ O ₄	203.0341	227.981	[M+H] ⁺
12	Auraptanol	C ₁₅ H ₁₆ O ₄	243.1021	228.050	[M+H] ⁺
13	Canthin-6-one	C ₁₄ H ₈ N ₂ O	221.0709	252.570	[M+H] ⁺
14	Xanthotoxin	C ₁₂ H ₆ O ₄	217.0496	258.389	[M+H] ⁺
15	Skimmianine	C ₁₄ H ₁₃ NO ₄	260.0917	266.435	[M+H] ⁺
16	Rutaevin	C ₂₆ H ₃₀ O ₉	487.1980	287.355	[M+H] ⁺
17	Isopimpinellin	C ₁₃ H ₁₀ O ₅	247.0605	335.763	[M+H] ⁺
18	N-methylflindersine	C ₁₅ H ₁₅ NO ₂	242.1177	401.860	[M+H] ⁺

KEGG pathway enrichment analysis was carried out using the DAVID on the 298 important targets, and 177 enriched KEGG entries were chosen if $P < 0.05$ was met. Figure 6D displays the bubble chart of the top 20 paths. The findings cover, among other things, the pathways involved in hsa05417: Lipid and atherosclerosis, hsa05200: Pathways in cancer, hsa04933: AGE-RAGE signaling pathway in diabetic complications, hsa05163: Human cytomegalovirus infection, hsa04620: Toll-like receptor signaling pathway, and hsa04668: TNF signaling pathway.

In the end, a “Couplet medicines-Serum prototype components-Key targets-Related pathways” network including 18 components, 15 targets, and 20 pathways was built using Chiplot (<https://www.chiplot.online/>), as shown in Figure 6E.

Validation of the Interaction Between Identified Compounds and Key Targets by Molecular Docking

During molecular docking investigations, four essential components (phellodendrine, xanthotoxin, nomilin, and isopimpinellin) were used as ligands. TNF, IL-6, IL-1 β , and AKT1 were the 4 core targets that were chosen as receptors for the molecular docking. If the binding energy is below 0 kcal/mol, the ligand can attach to the receptor on its own. A strong connection among the ligand and receptor is indicated by an affinity of less than or equal to -5 kcal/mol.²²

All key components exhibited binding energies below 0 kcal/mol, indicating their spontaneous affinity towards the receptor proteins. The majority of these constituents demonstrated binding energies lower than -5 kcal/mol, suggesting their effective binding to the core target proteins. From a molecular perspective, phellodendrine displayed the highest binding affinity with the core target proteins, followed by isopimpinellin. From a target standpoint, all four key compounds exhibited strong binding affinities with TNF and IL-6, highlighting these targets as crucial therapeutic targets for PC in AD treatment and suggesting that PC modulates inflammatory factor levels to address AD pathogenesis. Figure 7 shows the visualization results of docking with TNF and IL-6. The binding energies between the 4 main target proteins and the 4 essential components of PC are outlined in Table S3.

Experimental Verification Results

Utilizing network pharmacology and molecular docking techniques, our preliminary findings have underscored the critical involvement of TNF- α and IL-6 in the therapeutic landscape of AD. Recognizing the pivotal role these cytokines play in AD, we have embarked on a series of in vivo studies. Based on network pharmacology research, we have identified the TLR pathway as a pivotal pathway for treating AD with PC. As depicted in network pharmacology

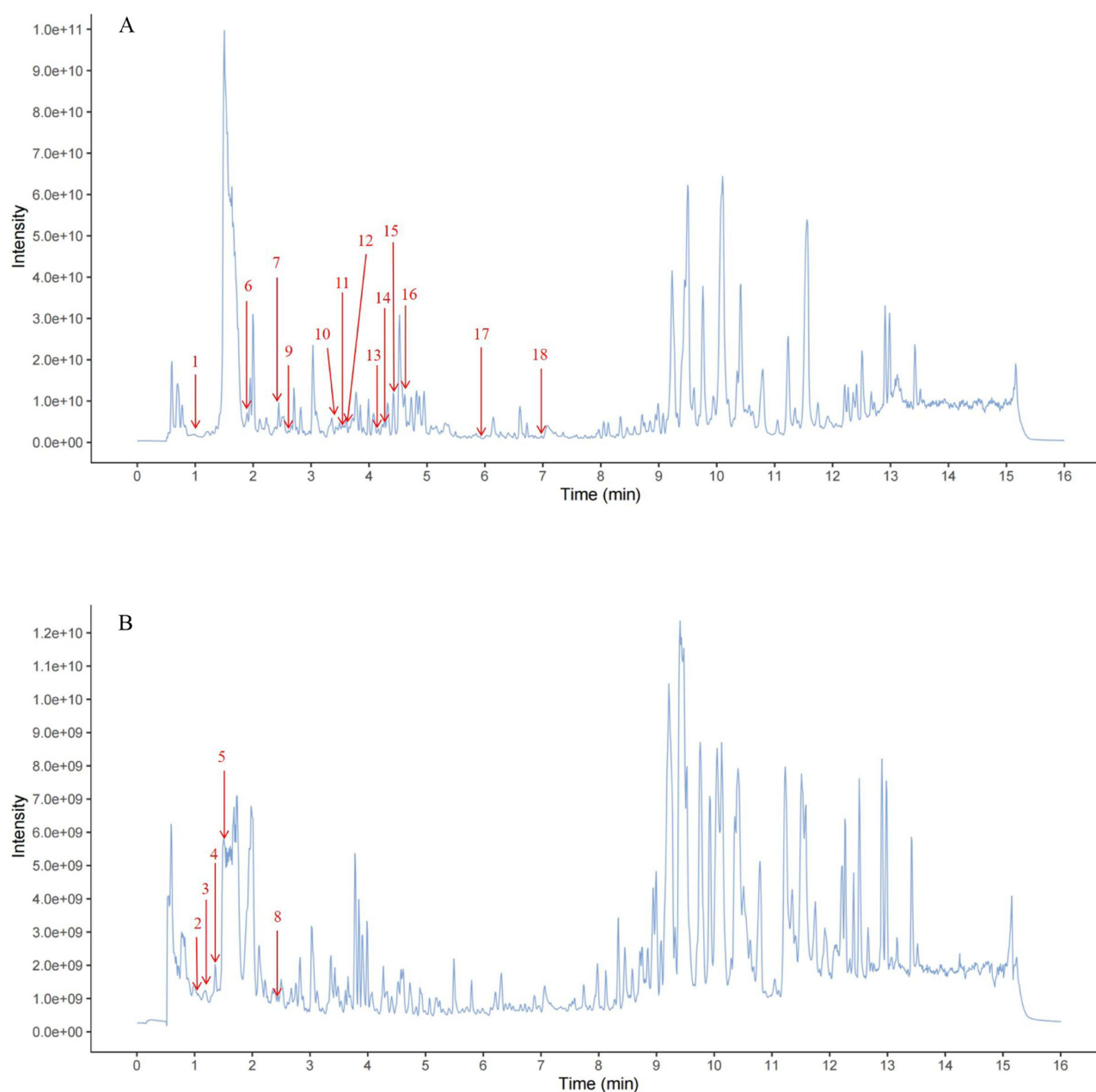


Figure 4 Total ion chromatograms of PC-treated mice serum. **(A)** Positive ion mode. **(B)** Negative ion mode.

research, TLR4 and NF- κ B emerged as crucial targets for AD treatment by PC. Expanding upon this investigation, we have assessed whether the anti-inflammatory effects of PC are mediated by the TLR4/NF- κ B pathway. These studies were expected to shed light on the molecular mechanisms by which these mediators contribute to the disease progression and potentially reveal new avenues for AD therapeutic intervention.

PC Ameliorated the Cutaneous Pathological Condition in Mice With AD

Figure 8A revealed that the control group displayed a normal architecture of the epidermis and dermis, displaying clear skin structure. In contrast, the model group demonstrated significant epidermal hyperplasia, hyperkeratosis, and acanthosis. The dermis presented marked edema and inflammatory cell infiltration. Following treatment with prednisolone and PC, there was a significant reduction in epidermal thickness, edema, and inflammatory cell infiltration. The PC-H group exhibited a decrease

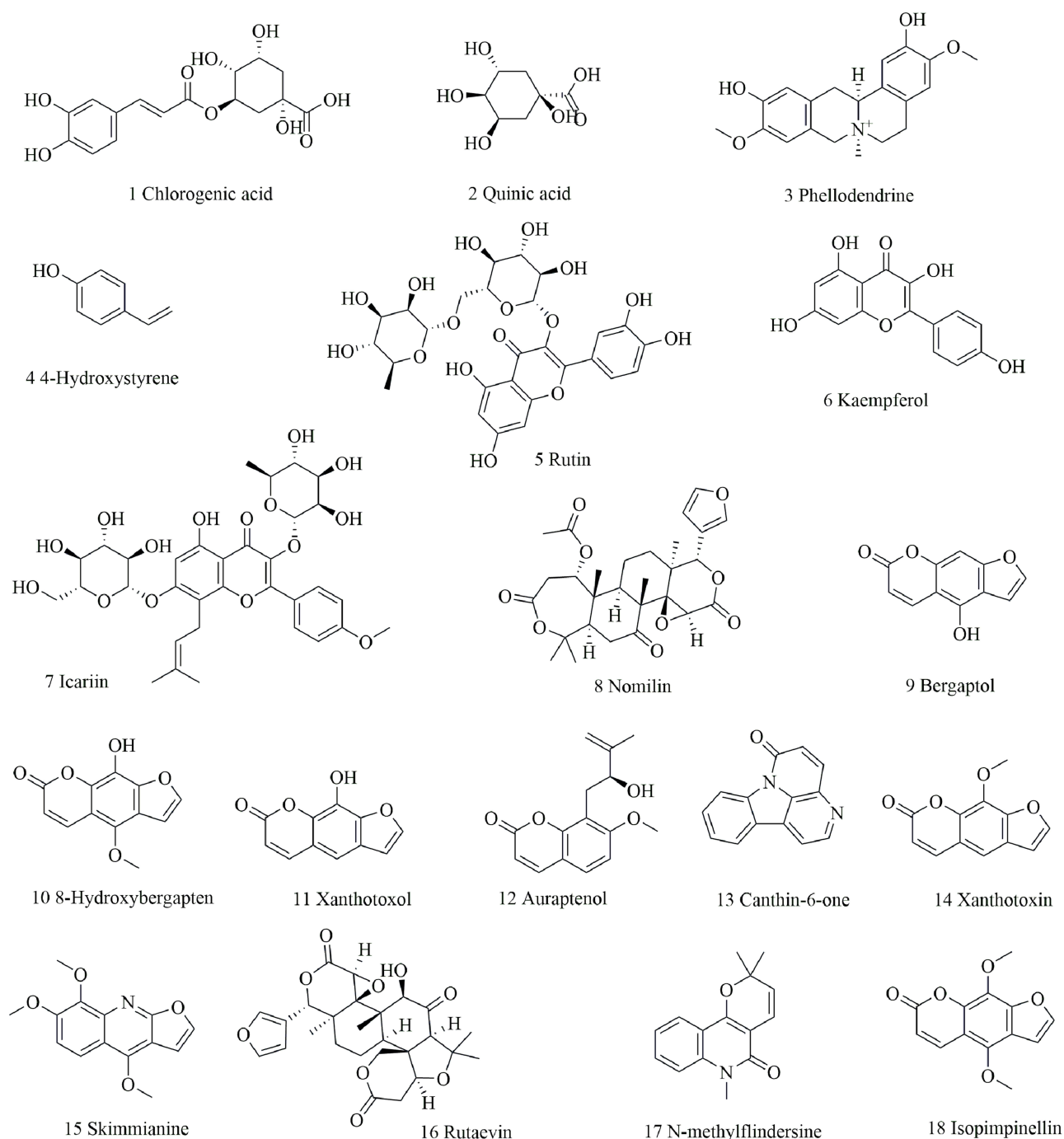


Figure 5 Structures of the serum prototype components.

in skin thickness comparable to that observed in the prednisolone group but more pronounced than those observed in the medium and low-dose groups.

PC Downregulated the Levels of IgE, IL-4, TNF- α and IL-6 in the Serum of AD Mice

We used ELISA kits to measure serum levels of IgE, IL-4, TNF- α , and IL-6 in AD mice with the goal to evaluate the impact of PC on these inflammatory cytokines. When contrasted with the control group, the model group showed a notable rise in serum IgE, IL-4, TNF- α , and IL-6 levels in mice ($P < 0.01$). In comparison to the model group, prednisolone and high-dose PC considerably reduced serum IgE levels, with statistically significant differences ($P < 0.01$). Although IgE levels in the PC-M

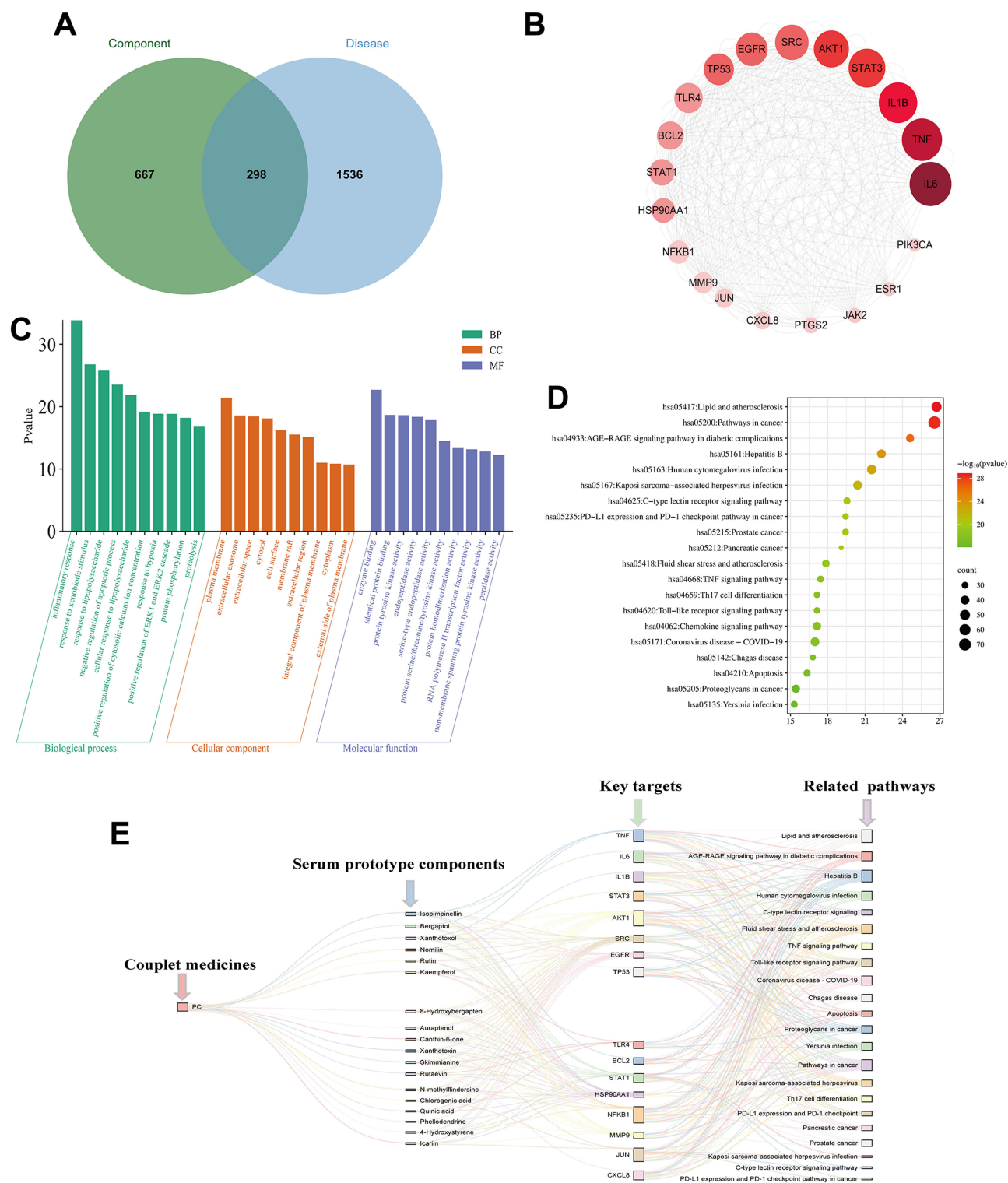


Figure 6 Network construction and analysis of PC treatment for AD. **(A)** Venn diagram of 965 potential targets from PC, 1834 AD-related targets, and 298 common targets. **(B)** PPI network of the 20 key targets. **(C)** The top 10 significantly enriched terms in GO analysis. **(D)** The top 20 significantly enriched terms in KEGG pathways. **(E)** The multivariate network of “Couplet medicines-Serum prototype components-Key targets-Related pathways”.

and PC-L groups revealed a downward trend, the variations were not statistically important ($P > 0.05$, Figure 8B). Both high and medium doses of PC and prednisolone were able to decrease the expression of IL-4, TNF- α and IL-6, with statistically significant differences compared to the model group ($P < 0.01$ or $P < 0.05$, Figure 8C-E). The low dose of PC showed no

Table 3 The Key Targets and Topological Parameters of PC in the Treatment of AD

Name	Degree	Betweenness Centrality	Closeness Centrality
IL-6	85	5222.2530	0.5309
TNF	81	7016.7260	0.5268
IL-1 β	73	4050.9731	0.5121
STAT3	72	2739.1396	0.4990
AKT1	70	3951.6882	0.5074
SRC	69	5722.4717	0.4991
EGFR	66	3409.3965	0.5027
TP53	63	2907.1160	0.4982
TLR4	60	3124.0476	0.4928
BCL2	57	3462.9932	0.4842

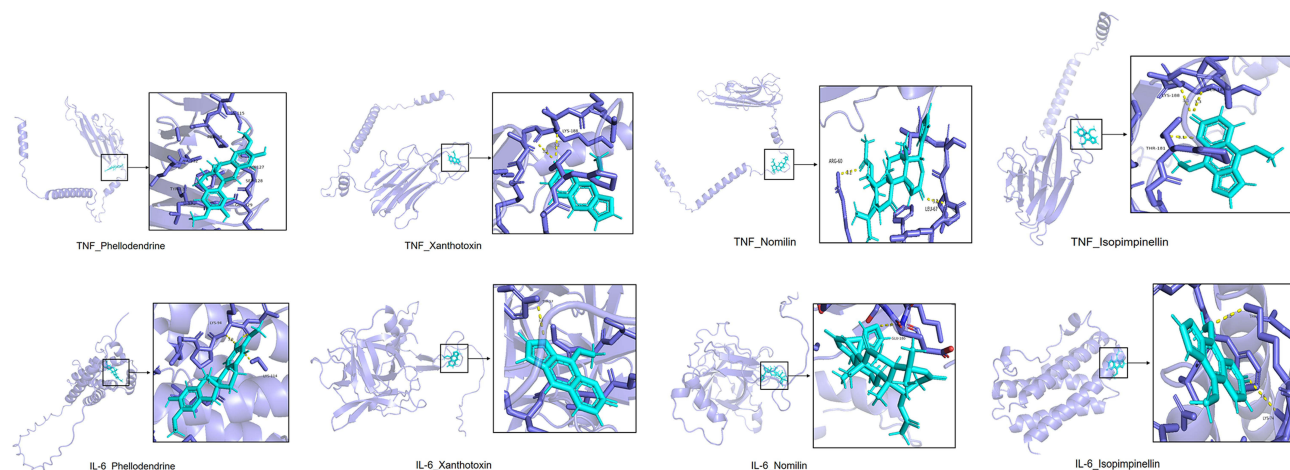
statistically significant difference from the model group ($P > 0.05$), suggesting that the effect of low-dose PC on reducing IL-4 is not pronounced.

PC Reduced the Levels of TNF- α and IL-6 in the Skin of AD Mice

In the IHC results, TNF- α and IL-6 positive cells were stained brown (Figure 9A). Compared to the control group, the expression of TNF- α and IL-6 in the skin tissues of the model group mice was significantly upregulated, with a statistically significant difference ($P < 0.01$). In comparison to the model group, the expression of TNF- α and IL-6 was markedly reduced in the PC-H group, PC-M group, and PC-L group, with statistical significance ($P < 0.01$ or $P < 0.05$, Figure 9B and C).

PC Influenced NF- κ B Nuclear Translocation

Nuclear translocation of NF- κ B is a crucial step in activating NF- κ B cascade.²⁶ As shown in Figure 10A, minimal co-localization between NF- κ B p65 and cell nucleus was observed in the control group, indicating weak fluorescence expression of NF- κ B p65. On the other hand, the DNCB-induced model group showed notable NF- κ B activation and nuclear translocation in contrast to the control group, marked by high levels of NF- κ B p65 fluorescence expression ($P < 0.01$, Figure 10B). Following PC intervention, nuclear translocation of NF- κ B was effectively suppressed as evidenced by reduced fluorescence expression of NF- κ B p65 ($P < 0.01$). Moreover, when comparing different dosage groups for PC treatment, it was found that high-dose PC showed weaker fluorescence expression and less co-localization with the cell nucleus than medium and low-dose groups. These findings

**Figure 7** The representative docking complex of important targets and components.

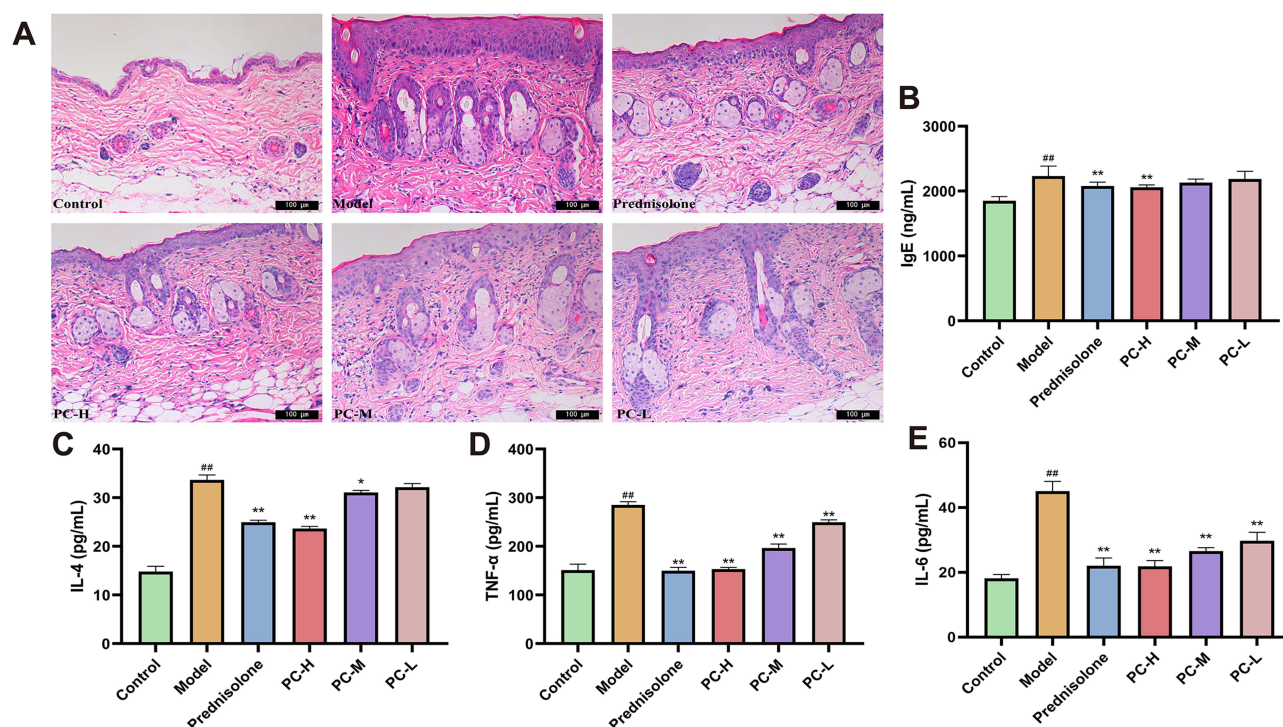


Figure 8 PC ameliorated dermal tissue pathology and serum inflammatory cytokine levels in AD mice. **(A)** Histological alterations in the skin tissue of AD mice. Representative H&E stained sections were showed (scale = 100 μ m, magnification \times 200). **(B–E)** Bar graphs of the levels of IgE, IL-4, TNF- α and IL-6 in each group. Data are presented as the mean \pm SD. ^{##} $P < 0.01$ vs control group. ^{*} $P < 0.05$, ^{**} $P < 0.01$ vs model group.

suggested that PC can suppress activation of NF- κ B within cell nucleus while alleviating inflammatory damage in AD, notably, high-dose PC demonstrated a more pronounced inhibitory effect than medium or low-dose groups.

Confirmation of PC's Regulatory Influence on the TLR4/NF- κ B Pathway

TLR4 and p-NF- κ B p65 protein expression levels were significantly higher in the skin tissues of mice in the model group than in the control group, according to Western blot data shown in Figure 11A–C. ($P < 0.01$). On the contrary, the level of I κ B- α protein expression substantially dropped ($P < 0.01$, Figure 11D). In contrast to the model group, both high- and medium-dose PC groups exhibited a significant reduction in TLR4 and p-NF- κ B p65 protein expression levels in skin tissues ($P < 0.01$), along with a notable increase in I κ B- α protein's expression level ($P < 0.01$). In the PC-L group, the mice's skin tissues showed a marked decrease in the expression level of p-NF- κ B p65 protein in the PC-L group ($P < 0.01$). The TLR4 protein expression level showed a declining tendency; however, this trend was not statistically notable ($P > 0.05$). Similarly, an increasing trend was observed in the expression level of I κ B- α protein; however, this also lacked statistical significance ($P > 0.05$). These findings suggested that high and medium doses of PC may effectively alleviate AD via preventing the TLR4/NF- κ B signaling pathway, with superior efficacy demonstrated by high-dose PC.

Discussion

TCM considers that AD arises from a constitutional predisposition to intolerance, with internal heat toxins lurking. External or internal injuries can trigger the dormant pathogenic factors, leading to the outward manifestation of heat toxins, the accumulation of damp-heat and turbidity in the skin, and a disharmony of qi and blood, which results in the disease. Phellodendri Chinensis Cortex is particularly known for its capacity to remove heat and dry dampness, and it also detoxifies and treats sores, making it an essential remedy for conditions such as boils, swellings, and eczema. Cnidii Fructus excels at drying dampness, expelling wind, killing parasites, and relieving itching, showing significant efficacy in treating damp dermatitis and severe sores. PC, tailored to the TCM syndrome of AD, synergistically achieves the effects of clearing heat and detoxifying, drying dampness, and killing parasites to alleviate itching. Both Phellodendri Chinensis

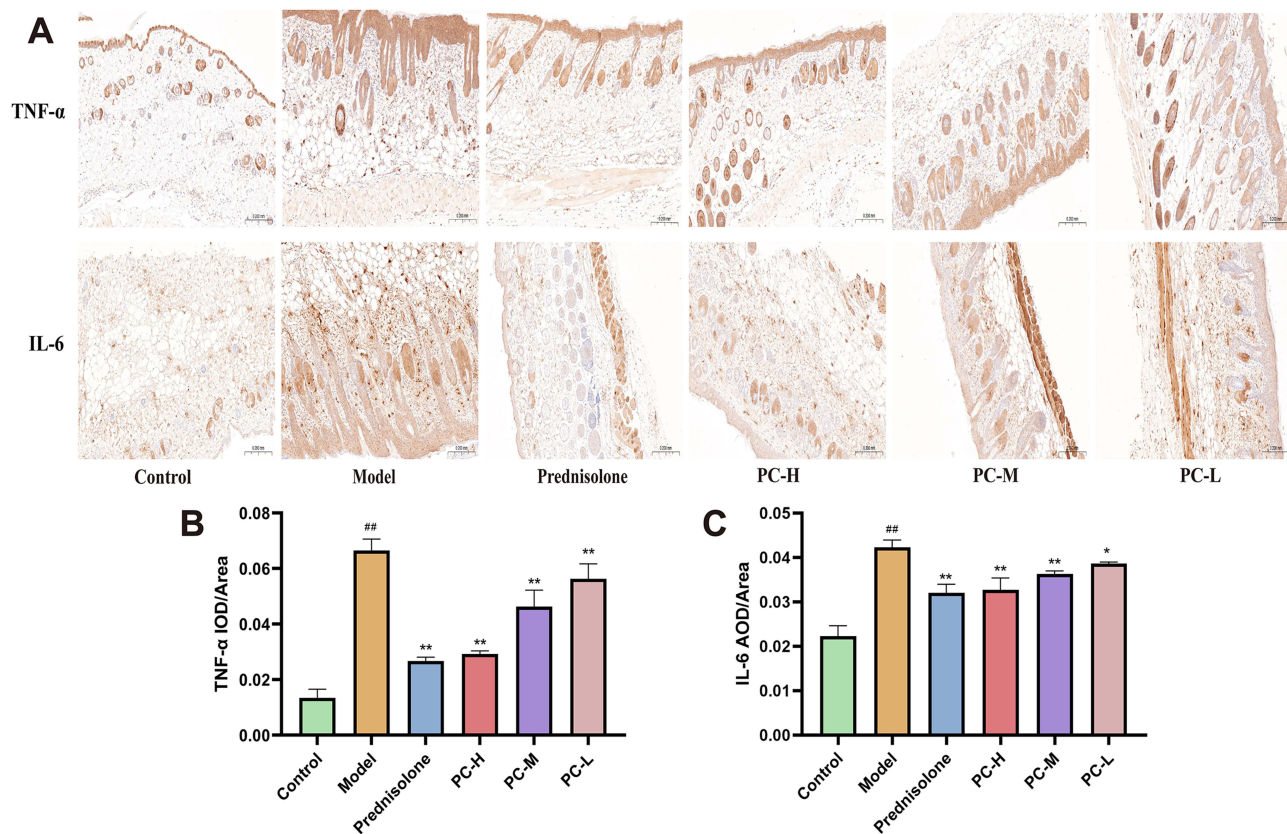


Figure 9 Impact of PC on the expression of TNF- α and IL-6 in the skin of AD mice. **(A)** Skin tissue sections were stained with IHC. Representative skin tissue sections (scale = 200 μ m, magnification \times 200) were stained. **(B and C)** Expression of TNF- α and IL-6 in skin. Data are presented as the mean \pm SD. ^{##} $P < 0.01$ vs control group. ^{*} $P < 0.05$, ^{**} $P < 0.01$ vs model group.

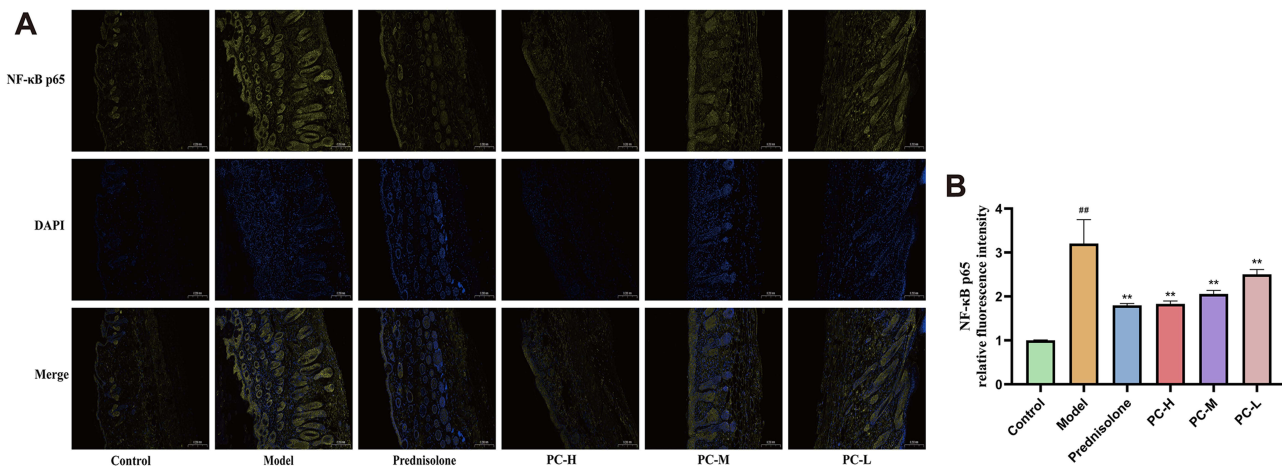


Figure 10 The effect of PC on NF- κ B nuclear translocation. **(A)** The fluorescence images of NF- κ B p65 in each groups (scale = 200 μ m, magnification \times 200). **(B)** Bar graph of NF- κ B p65 relative fluorescence intensity in each group. Data are presented as the mean \pm SD. ^{##} $P < 0.01$ vs control group. ^{**} $P < 0.01$ vs model group.

Cortex and Cnidii Fructus possess modern pharmacological effects of anti-inflammation and antimicrobial activity, making them suitable for the management of inflammatory skin disorders, including AD.^{10,14} Existing research has demonstrated that the herb pair composed of Phellodendri Chinensis Cortex and Cnidium Fructus can reduce the levels of IgE and TNF- α in mice with eczema, decrease the scratching behavior in itchy mice, and possess significant anti-inflammatory and antipruritic effects.²⁷ As previously discussed in the introduction, clinical studies have demonstrated

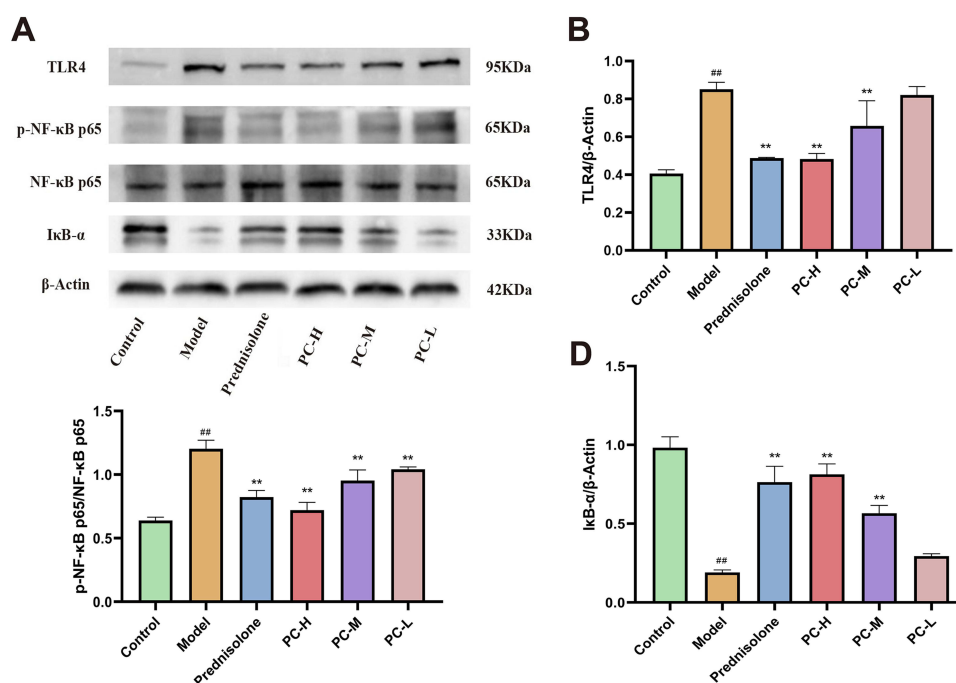


Figure 11 Effect of PC on the expression of inflammatory-related proteins. **(A)** Content of TLR4, p-NF-κB p65, NF-κB p65, and IκB-α were detected by Western blot. **(B-D)** Bar graphs of the relative expressions of TLR4, p-NF-κB p65, and IκB-α in each group. Data are presented as the mean ± SD. ^{###}*P*<0.01 vs control group. ^{**}*P*<0.01 vs model group.

that the combination of PC with Western medications such as pevisone significantly outperforms monotherapy with Western medications in alleviating eczema-like symptoms of AD. This combination therapy exhibits a higher efficacy rate in controlling pruritus and skin lesions compared to Western medications alone. Moreover, PC has been shown to possess favorable safety profiles with a low incidence of adverse reactions. In terms of reducing relapse rates, PC is markedly superior to representative corticosteroid drugs such as hydrocortisone butyrate and pevisone.^{18–20} These clinical findings provide a robust theoretical foundation for our experimental investigation and have motivated us to further explore the pharmacodynamic constituents and underlying mechanisms of PC in the treatment of AD. This exploration aims to uncover its broader potential for clinical application and to elucidate the mechanisms through which PC achieves its therapeutic effects.

Understanding the chemical foundation of PC is crucial for the therapeutic integration of PC. This study employed UPLC-MS technology for qualitative analysis of the components in the aqueous extract of PC. The 53 compounds identified from the PC aqueous extract broadly encompass the primary active components of *Phellodendri Chinensis Cortex* and *Cnidium Fructus*, including 11 alkaloids (berberine, berberrubine, palmatine, dehydroevodiamine, skimmianine, phellodendrine, magnoflorine, jatrorrhizine, γ -fagarine, N-methylflindersine, and canthin-6-one), 14 coumarins (osthole, bergapten, bergaptol, imperatorin, isoimperatorin, isopimpinellin, 7-demethylsuberosin, xanthotoxin, xanthoxol, auraptanol, fraxetin, and 8-hydroxybergapte), 4 limonoids (rutaevin, obacunone, limonin, and nomilin), 6 flavonoids (kaempferol, quercetin, rutin, hesperidin, hyperoside, and icariin), 3 chromones (5-O-methylvisammioside, cimifugin, and noreugenin), 5 phenolic acids (quinic acid, ferulic acid, chlorogenic acid, caffeic acid, and isochlorogenic acid B), as well as 10 other compounds (stigmasterol, linoleic acid, oleic acid, 4-hydroxystyrene, styrene, perillene, coniferin, anisic aldehyde, 5-hydroxymethylfurfural, and cassiastearoptene). Notably, previous research has primarily focused on the quantitative analysis of a limited number of constituents such as berberine, magnoflorine, cnidilin, and zanthotoxine.²⁸ However, these studies have not provided a comprehensive qualitative characterization of the full chemical profile of PC. Our study fills this gap by identifying a diverse array of chemical components, thereby offering a more holistic understanding of the pharmacological basis of PC. This comprehensive qualitative analysis not only provides essential reference data for the subsequent quality control of PC but also lays the groundwork for identifying

key pharmacodynamic substances. Future research should focus on elucidating the specific mechanisms of action of these identified compounds, particularly their roles in anti-inflammatory and antimicrobial activities, which are critical for managing inflammatory skin disorders such as AD.

Guided by the theory of serum pharmacology, based on the aforementioned research, a comparison was made between the drug-containing serum chromatogram and the water-decocted liquid chromatogram, resulting in the identification of 18 prototype components absorbed into the serum. These components include alkaloids, coumarins, limonoids, flavonoids, and phenolic acids, specifically chlorogenic acid, quinic acid, phellodendrine, 4-hydroxystyrene, rutin, kaempferol, icariin, nomilin, bergaptol, 8-hydroxybergapten, xanthoxol, auraptinol, canthin-6-one, xanthotoxin, skimmianine, rutaevin, isopimpinellin, and N-methylflindersine. Current research on the components of PC that enter the bloodstream is relatively scarce, with a focus on the exploration of components absorbed into the bloodstream from single herbs such as *Phellodendri Chinensis Cortex* and *Cnidium Fructus*. Studies on the components of *Phellodendri Chinensis Cortex* that enter the bloodstream have mostly concentrated on alkaloids.^{29,30} This study found that, in addition to alkaloids, prototype components of the *Phellodendri Chinensis Cortex* that enter the bloodstream also include limonoids such as nomilin. The identified components of *Cnidium Fructus* that enter the bloodstream include coumarins such as xanthotoxin and Isopimpinellin.³¹ This study discovered that, in addition to the aforementioned components, other coumarin compounds such as bergaptol and xanthoxol are also found among the prototype components from *Cnidium Fructus* that enter the bloodstream in the PC. Research indicates that phellodendrine mitigated myocardial injury by activating Nrf2 pathway and concurrently inhibiting NF- κ B pathway, thereby reducing the levels of TNF- α and IL-6 in cardiac tissue and enhancing antioxidant and anti-inflammatory capabilities of the myocardium.³² Furthermore, it can also alleviate bacterial mucosal lesions by reducing the levels of IL-1 β , IL-6, IL-8, and TNF- α .³³ Alkaloidal PC constituents may slow the progression of AD by exerting anti-inflammatory and antimicrobial activities. Xanthoxol has been demonstrated to inhibit the NLRP3 protein and the NF- κ B pathway, thereby downregulating IL-1 β , IL-6, and TNF- α expression, for the treatment of osteoarthritis.³⁴ Nomilin can alleviate inflammatory responses by suppressing TLR4/NF- κ B pathway and downregulating the levels of *Klebsiella pneumoniae*-induced cytokines IL-6, IL-1 β , and TNF- α .³⁵ Xanthotoxin, isopimpinellin and bergaptol inhibited the pro-inflammatory cytokines TNF- α and IL-6 and upregulated the anti-inflammatory cytokine IL-10 by suppressing the Janus kinase (JAK)/STAT signaling pathway, thus demonstrating anti-inflammatory properties.³⁶ Chlorogenic acid significantly reduces the expression of MMP-9 and HSP90AA1 mRNA, as well as gene expression associated with the TNF pathway, including TNF- α , tumor necrosis factor receptor 1 (TNFR1), and AKT1.³⁷ Collectively, these findings have indicated that the identified prototype components, such as phellodendrine, xanthoxol, nomilin, xanthotoxin, isopimpinellin, and bergaptol, form the material basis for PC's anti-inflammatory and antimicrobial activities. However, their specific roles in AD remain to be elucidated and will be a focus of future investigations. This study not only provides essential reference data for the quality control of PC but also lays the groundwork for identifying key pharmacodynamic substances and their mechanisms of action in the management of inflammatory skin disorders.

This study acquired chemicals and targets from approved databases and conducted PPI assessment on the intersection of serum prototype components and disease-related targets, yielding key targets such as TNF, IL-6, and TLR4. These targets are thought to be the primary focus of PC in the management of AD. Cytokines such as TNF and IL-6 are polypeptides or proteins that play significant regulatory roles within the immune system. The TNF superfamily consists of 19 members, with TNF- α being an important one. TNF- α is typically produced by macrophages and activates signaling pathways such as NF- κ B, participating in the induction of inflammation and being significantly associated with the occurrence of diseases like rheumatoid arthritis, inflammatory bowel disease, and psoriasis.³⁸ IL-6 is secreted by activated T cells and released during skin reactions in atopic patients following an allergen challenge, with dendritic cells in atopic patients also producing excessive IL-6. TLR4, as an amplifier of inflammatory responses, is crucial in the development of AD; its activation and regulation of inflammatory cytokines are released as a result of NF- κ B signaling.³⁹

Network pharmacology was employed to predict that the treatment of AD with PC may be connected to signaling pathways like TLR pathway. TLRs play a crucial role in the innate immune system, recognizing microbes that breach physical barriers like the skin and activating immune cells such as macrophages, thereby initiating immune responses. TLR4/NF- κ B signaling pathway is an important route at our body's immune system, which is involved in the occurrence

and regulation of various diseases, including autoimmune, inflammatory, and allergic diseases. Upon activation, TLR4 initiates a series of actions that lead to NF- κ B signaling pathway being activated. This, in turn, drives the creation of key inflammatory cytokines, including TNF- α and IL-6. The subsequent surge in these pro-inflammatory cytokines is linked to pruritus exacerbation and inflammatory responses observed in patients with AD, underscoring the significance of TLR4/NF- κ B signaling in the pathophysiology of the disease. Chinese medicine and its extracts have been demonstrated to treat AD by regulating the TLR4/NF- κ B signaling pathway. Our preliminary research has confirmed the efficacy of the *Sophora flavescens*-*Angelica sinensis* herbal pair in inhibiting the TLR4/NF- κ B pathway.⁴⁰ Additionally, studies have indicated that the herbal extract of ursolic acid downregulates the TLR4/NF- κ B pathway to suppress AD progression.⁴¹ These findings indicate that the network pharmacology predictions of this study have some credibility, suggesting that PC can treat AD by modulating the TLR4/NF- κ B pathway.

The reliability of network analysis is critical issue that we greatly value. Therefore, we explored the regulatory effects of PC on inflammatory responses and TLR4/NF- κ B signaling pathway using techniques such as ELISA, IHC, IF, and Western blot to verify the predictions made by network pharmacology. This study used the topical application of DNCB to induce an AD model. The modeling results indicated that after the procedure, the mice exhibited significant restlessness, skin redness, swelling, crusting, and scaling, accompanied by pronounced itching, which are consistent with the symptoms of AD, suggesting successful modeling. After treatment with PC, the acute inflammatory responses of the skin lesions on the backs of the mice gradually resolved, demonstrating a significant inhibitory effect of PC on AD. Interestingly, the high dose of PC's effectiveness was on par with the prednisolone group's, with the high dose showing superior effects over the medium and low doses. Elevated levels of IgE represent a characteristic feature in the pathogenesis of AD. The cross-linking between IgE and Fc-epsilon receptor (Fc ϵ R) on mast cells triggers their activation, thereby initiating inflammation through the release of mediators like histamine and tryptase. IL-4, a pro-inflammatory cytokine secreted by Th2 cells, plays a crucial role in allergic inflammatory responses mediated by IgE, with its levels escalating progressively throughout the course of the disease. The experimental results revealed that the model group mice had obvious epidermal hyperplasia, acanthosis, severe dermal edema, and inflammatory cell infiltration; the levels of IL-4 and IgE in the serum were mostly elevated. Following treatment with PC, the levels of serum IL-4 and IgE in the mice were notably reduced, and the itching symptoms were alleviated. This suggested that PC may modulate the immune response by intervening in cytokine regulation, thereby alleviating the symptoms of AD. The pleiotropic cytokine IL-6 activates IL-4 production of CD4⁺ T cells, inducing the acute-phase response in AD, and elevated levels can lead to immune-mediated pathological damage. TNF- α is a pro-inflammatory cytokine and a key initiator of antimicrobial inflammatory responses.⁴² ELISA and IHC detection of TNF- α and IL-6, which are closely related to the pathogenesis of AD, showed that PC markedly decreased TNF- α and IL-6 expression in AD mice. TLR4 is an upstream key factor in the immune system, with its expression gradually increasing from the basal layer to the upper spinous layer in AD patients.⁴³ NF- κ B is an inducible transcriptional regulator located downstream of the TLR4 signaling pathway. When not activated, NF- κ B and its corresponding inhibitor I κ B exist in the cytoplasm in a bound state. Upon stimulation by extracellular signals such as pro-inflammatory factors, I κ B undergoes self-ubiquitination and proteasomal degradation, allowing NF- κ B to translocate from the cytoplasm to the nucleus, activating the NF- κ B signaling pathway and promoting the release of pro-inflammatory factors TNF- α and IL-6.⁴⁴ After treatment with PC, the fluorescence expression of NF- κ B p65 in mouse skin tissue was weakened, and the co-localization with the cell nucleus was significantly reduced, indicating that PC can alleviate AD inflammation by inhibiting the stimulation of NF- κ B and downregulating the expression of NF- κ B in cell nucleus. In the high and medium dose groups of PC, the protein expression of TLR4 and p-NF- κ B p65 in mouse skin tissue were significantly reduced, and the protein expression of I κ B- α was considerably increased. In the mechanistic study of PC, we found that PC could mitigate AD symptoms by inhibiting the TLR4/NF- κ B signaling pathway. This inhibition was achieved by reducing the levels of TLR4 and p-NF- κ B p65 proteins, and by preventing the breakdown of I κ B- α , a key inhibitory protein. It is noteworthy that the high dosage of PC demonstrates superior efficacy compared to medium and low dosages, potentially due to the anti-inflammatory and itch-relieving effects of PC being closely associated with the content of its alkaloids and coumarins.

Compared with existing therapies, PC represents a holistic approach rooted in TCM, characterized by its multi-target and multi-pathway mechanisms. Unlike conventional treatments that primarily target single pathways or cytokines (eg,

IL-4R α for dupilumab or JAK inhibitors), PC integrates multiple antimicrobial and anti-inflammatory active ingredients and carries out its traditional role of clearing heat, drying dampness and relieving itching through the TLR4/NF- κ B signaling pathway and targets including IgE, IL-4, and TNF- α for targeting multiple pathologic aspects of AD. This multi-faceted approach may provide a more comprehensive therapeutic effect for AD. Moreover, PC offers a potentially more cost-effective alternative to existing therapies, such as immunosuppressants or biologics, especially for long-term management. This is particularly relevant given the high costs and potential long-term side effects associated with current treatments. The holistic nature of PC allows for personalized adjustments based on individual symptoms and disease progression, which is a significant advantage over standardized biologic therapies.

However, this study does have some limitations. First, it has been established that the TLR4/NF- κ B pathway is a new therapy avenue for AD. Beyond TLR4 and NF- κ B, the impact of other targets on this pathway remains not fully elucidated. Our preliminary *in vivo* experiments have explored the mechanisms underlying the therapeutic effects of PC on AD, revealing that its efficacy is dosage-dependent. Future research will integrate *in vitro* cell experiments to further elucidate these mechanisms. Additionally, toxicology studies will be conducted to determine the optimal dosage of PC that ensures both safety and efficacy, thereby optimizing clinical treatment protocols. Although the potential substance basis for the therapeutic effects of PC on AD has been identified, further investigation is required to pinpoint the specific active ingredients. Monomer therapy experiments are planned to clarify the contributions of individual active components. These issues will be systematically addressed in our future in-depth research endeavors. In summary, this study comprehensively investigated the potential active ingredients, molecular targets, and signaling pathways involved in the therapeutic effects of PC on AD by integrating serum pharmacology, network pharmacology, and experimental validation. Our findings indicated that PC exerts its therapeutic effects on AD primarily through the inhibition of inflammatory reactions. Specifically, we have demonstrated that the TLR4/NF- κ B signaling cascade is a central mediator in resolving the inflammatory processes associated with AD. This study not only elucidates the molecular mechanisms underlying the therapeutic actions of PC but also provides a foundation for identifying novel therapeutic targets and strategies for the management of AD.

Conclusion

The current data indicated that the 18 identified prototype components absorbed into the bloodstream (chlorogenic acid, quinic acid, phellodendrine, 4-hydroxystyrene, rutin, kaempferol, icariin, nomilin, bergaptol, 8-hydroxybergapten, xanthotoxol, auraptenol, canthin-6-one, xanthotoxin, skimmianine, rutaevin, isopimpinellin, and N-methylflindersine) may constitute the pharmacological foundation for PC's therapeutic effect against AD, especially phellodendrine, xanthotoxin, nomilin, and isopimpinellin. The primary mechanism of PC in treating AD was suggested to involve targeting the TLR4/NF- κ B signaling pathway, downregulating the levels of inflammatory cytokines including IgE, IL-4, TNF- α , and IL-6, thereby alleviating AD-associated inflammation. In this study, PC demonstrated dose-dependent efficacy in treating AD, with high doses achieving therapeutic effects comparable to prednisolone but with fewer side effects. These findings suggest that PC is a safe and effective alternative therapy with significant clinical potential. Our research has laid the groundwork for further exploration of PC's active components and therapeutic mechanisms, providing preclinical evidence for its efficacy in AD treatment. Additionally, our results may inform the rational clinical application of PC in managing AD. Given the complex nature of traditional Chinese herbal medicine, characterized by its multiple components and targets, future research should focus on elucidating the mechanisms of action of PC and optimizing its clinical application.

Abbreviations

AD, atopic dermatitis; AKT, protein kinase B; BP, biological process; CC, cell component; CLDN, claudin; DNCB, 2,4-dinitrochlorobenzene; EIF3F, eukaryotic translation initiation factor 3F; Fc ϵ R, Fc-epsilon receptor; GO, Gene Ontology; ICAM-1, intercellular adhesion molecule-1; IF, immunofluorescence; IFN- γ , interferon- γ ; IgE, immunoglobulin E; IHC, immunohistochemistry; IL-4, interleukin-4; JAM, junctional adhesion molecule; KEGG, Kyoto Encyclopedia of Genes and Genomes; MALT1, mucosa-associated lymphoid tissue lymphoma translocation gene 1; MF, molecular function; MIF, macrophage migration inhibitory factor; NF- κ B, nuclear factor- κ B; PC, Phellodendri Chinensis Cortex-Cnidii Fructus; PGRN, progranulin; PI3K, phosphatidylinositol 3-kinases; PPI, protein-protein interaction; STAT5, signal transducer and activator of transcription 5; TCM, traditional Chinese medicine; TLR4, Toll-like

receptor 4; TNF- α , tumor necrosis factor- α ; UPLC-MS, ultra performance liquid chromatography-mass spectrometry; VCAM-1, vascular endothelial cell adhesion molecule-1; ZO, zonula occludens.

Data Sharing Statement

The data used to support the findings of this study are included within the article.

Ethics Statement

This animal experiment was examined and approved by the Ethics Review Committee for the Welfare of Experimental Animals at Shandong University of Traditional Chinese Medicine and was conducted in compliance with the Animal Experiment Ethics Code 2022-7 (approval number: SDUTCM20230228001).

Funding

This project is aided by Qilu febrile Disease School Tongfu Syndrome differentiation and treatment of febrile Diseases TCM characteristic Technology (LuWei Letter [2022] 93); Qilu authentic Medicine processing Technology (LuWei Letter [2021] 45); Shandong Province Graduate Education Quality Courses and Professional Degree Graduate Teaching Case Base Project (No. SDYAL20053); Shandong Province Graduate Education Quality Improvement Program (No. SDYKC21047).

Disclosure

The authors declare no conflicts of interest.

References

- Kim KW, Koh SJ, Kang HW, et al. Atopic dermatitis is associated with the clinical course of inflammatory bowel disease. *Scand J Gastroenterol.* 2023;58(10):1115–1121. doi:10.1080/00365521.2023.2209688
- Chu DK, Koplin JJ, Ahmed T, Islam N, Chang CL, Lowe AJ. How to prevent atopic dermatitis (eczema) in 2024: theory and evidence. *J Allergy Clin Immunol Pract.* 2024;12(7):1695–1704. doi:10.1016/j.jaip.2024.04.048
- Silverberg JI. Adult-onset atopic dermatitis. *J Allergy Clin Immunol Pract.* 2019;7(1):28–33. doi:10.1016/j.jaip.2018.09.029
- Barbarot S, Auziere S, Gadkari A, et al. Epidemiology of atopic dermatitis in adults: results from an international survey. *Allergy.* 2018;73(6):1284–1293. doi:10.1111/all.13401
- Ochayon DE, DeVore SB, Chang WC, et al. Progressive accumulation of hyperinflammatory NKG2D(low) NK cells in early childhood severe atopic dermatitis. *Sci Immunol.* 2024;9(92):eadd3085. doi:10.1101/2023.06.02.23290884
- Hill DA, Spergel JM. The atopic march: critical evidence and clinical relevance. *Ann Allergy Asthma Immunol.* 2018;120(2):131–137. doi:10.1016/j.anai.2017.10.037
- Vandewalle J, Luypaert A, De Bosscher K, Libert C. Therapeutic mechanisms of glucocorticoids. *Trends Endocrinol Metab.* 2018;29(1):42–54. doi:10.1016/j.tem.2017.10.010
- Gu GG. *Shen Nong Ben Cao Jing*. Beijing: People's Medical Publishing House; 1956. Chinese.
- Chinese Pharmacopoeia Commission. *Pharmacopoeia of the People's Republic of China 2020* Chinese. Beijing: China Medical Science and Technology Press; 2020.
- Sun Y, Lenon GB, Yang AWH. Phellodendri cortex: a phytochemical, pharmacological, and pharmacokinetic review. *Evid Based Complement Alternat Med.* 2019;2019:7621929. doi:10.1155/2019/7621929
- Jiang YQ, Hu Y, Wu YX, Zhou XJ. The effect of phellodendri chinensis cortex on granule protein precursor in eczema mice. *Lab Med Clin.* 2023;20(10):1467–1469. doi:10.3969/j.issn.1672-9455.2023.10.029
- Andoh T, Yoshihisa Y, Rehman MU, Tabuchi Y, Shimizu T. Berberine induces anti-atopic dermatitis effects through the downregulation of cutaneous EIF3F and MALT1 in NC/Nga mice with atopy-like dermatitis. *Biochem Pharmacol.* 2021;185:114439. doi:10.1016/j.bcp.2021.114439
- Dai YQ, Du CM, Xie HP. Intervention effect of Huangbai capsule combined with olopatadine hydrochloride on acute eczema model rats and its anti-allergic mechanism. *Mod J Int Tradit Chin Med.* 2021;30(9):926–930,1005. doi:10.3969/j.issn.1008-8849.2021.09.004
- Sun Y, Yang AWH, Lenon GB. Phytochemistry, ethnopharmacology, pharmacokinetics and toxicology of cnidium monnieri (L.) Cusson. *Int J mol Sci.* 2020;21(3). doi:10.3390/ijms21031006
- Yao BH, Wang JX, Yao MY, Ran ZL. Effects of shechuangzi san on Th1/Th2 immune function in eczema rats. *World Sci Technol Mod Tradit Chin Med Mater Med.* 2024;26(5):1328–1335. doi:10.11842/wst.20230727010
- Chen JR, Hong XP, Duan YJ, Zhang YH, Han YM. The effect of osthole extract on skin barrier and chronic itching in mice with specific dermatitis. *Chin Tradit Pat Med.* 2021;43(12):3489–3492. doi:10.3969/j.issn.1001-1528.2021.12.045
- Xiong J, Zhong ZD, Fu R, Xiong W. Effect of osthole on mast cells and expression of STAT5 gene and protein in mice with eczema. *Herald Med.* 2015;34(12):1584–1587. doi:10.3870/j.issn.1004-0781.2015.12.009
- Jiang W, Zhai XX. Observation on the therapeutic effect of Shedu Xifang fumigation and washing method on perianal eczema. *Fujian J Tradit Chin Med.* 2018;49(3):22–24.

19. Wen BB. 2019. *Clinical Observation and Immunological Mechanism Analysis of Huangdi Decoction in Treating Baby Eczema*. Nanchang: Nanchang University, Chinese.
20. Gao ZP, Ai RD, Hao PS. Observational study on the short-term efficacy of shehuang ointment in the external treatment of 60 cases of subacute eczema. *Chin J Inf Tradit Chin Med*. 2007;14(3):57. doi:10.3969/j.issn.1005-5304.2007.03.030
21. Zhao X, Su H, Chen H, et al. Integrated serum pharmacology and network pharmacology to explore the mechanism of Yi-Shan-Hong formula in alleviating chronic liver injury. *Phytomedicine*. 2024;128:155439. doi:10.1016/j.phymed.2024.155439
22. Chen M, Zhong G, Liu M, et al. Integrating network analysis and experimental validation to reveal the mitophagy-associated mechanism of Yiqi Huoxue (YQH) prescription in the treatment of myocardial ischemia/reperfusion injury. *Pharmacol Res*. 2023;189:106682. doi:10.1016/j.phrs.2023.106682
23. Zhang Y. *Study on the Mechanism of Active Ingredients Composition of Danzhi Longdan Xiaoyao Decoction on Atopic Dermatitis*. Wuxi: Jiangnan University; 2021. Chinese.
24. Lee Y, Choi HK, N'Deh KPU, et al. Inhibitory effect of centella asiatica extract on DNCB-induced atopic dermatitis in HaCaT cells and BALB/c mice. *Nutrients*. 2020;12(2). doi:10.3390/nul2020411
25. Wang YJ. *Effect and Mechanism of Bisdemethoxycurcumin on Atopic Dermatitis*. Changchun, Jilin University; 2022. Chinese
26. Guo DK, Zhu Y, Sun HY, et al. Pharmacological activation of REV-ERBa represses LPS-induced microglial activation through the NF-κB pathway. *Acta Pharmacol Sin*. 2019;40(1):26–34. doi:10.1038/s41401-018-0064-0
27. Yu ZJ, Deng T, Li JS, Xu Y, Chen ML, Sun T. Research on anti-allergic, antipruritic and anti-inflammatory effects of Shehuang ointment on eczema. *Chin J New Drug*. 2020;29(16):1868–1876.
28. Tian B, Zhai XL, Lin YP, Yuan QH, Song Y. Determination of the content of components in the Phellodendron-Cnidium medicinal pair using a multi-wavelength switching HPLC method. *J Chin Med Mater*. 2020;43(8):1952–1955. doi:10.13863/j.issn1001.4454.2020.08.029
29. Kang LX, Xu ZP, Liu Y, Yang J, Yang BY, Kuang HX. Identification of prototype components and their metabolites in rat serum, urine and feces after oral administration of phellodendri amurensis cortex aqueous extract by UPLC-orbitrap fusion lumos tribrid-MS. *Chin J Exp Tradit Med Form*. 2021;27(11):139–146. doi:10.13422/j.cnki.syfjx.20211050
30. Feng QQ. *Analysis of Serum and Urine Metabolites of Phellodendron Amurense and Its Active Ingredients*. Haerbin, Heilongjiang University of Chinese Medicine; 2012. Chinese.
31. Song GS. *Based on Chromatographic Hypenated Technology for the Simultaneous Analysis of Multiple Components in Cnidium Monnieri and Its Compound Preparations, and the Study of Drug Metabolism and Pharmacokinetics*. Shijiazhuang, Hebei Medical University; 2015. Chinese.
32. Yang K. Effects of phellodendrine on antioxidation and inflammation in rats after overload exercise. *mol Plant Breed*. 2023;21(12):4109–4115. doi:10.13271/j.mpb.021.004109
33. Zhang DM, Li HJ, Zhou Q. Protective effect of phellodendrine on bacterial vaginosis mice. *Chin Tradit Herbal Drugs*. 2018;49(24):5849–5853. doi:10.7501/j.issn.0253-2670.2018.24.018
34. Zhuang ZM, Wu ZM, Ke GS, Ding JH. Xanthotoxol against knee osteoarthritis in rats by inhibiting inflammation: an experimental study. *Military Med Sci*. 2019;43(10):767–771. doi:10.7644/j.issn.1674-9960.2019.10.008
35. Liu ZM, Sun Y, Gao YC, Long HC, Lei T, Du HJ. Effects of Nomilin on inflammatory response in Klebsiella-induced geriatric pneumonia rats. *Chin J Immunol*. 2019;35(8):970–975. doi:10.3969/j.issn.1000-484X.2019.08.016
36. Perri MR, Pellegrino M, Aquaro S, et al. Cachrys spp. from southern Italy: phytochemical characterization and JAK/STAT signaling pathway inhibition. *Plants (Basel)*. 2022;11(21). doi:10.3390/plants11212913
37. Nie WK, Xu Y, Yu ZR, Yang HW, Liu B, Wang GX. Study on mechanisms of chlorogenic acid in treating atopic dermatitis based on network pharmacology. *J Guangdong Pharm Univ*. 2024;40(2):91–103. doi:10.16809/j.cnki.2096-3653.2023120601
38. Ma Q, Hao S, Hong W, et al. Versatile function of NF-κB in inflammation and cancer. *Exp Hematol Oncol*. 2024;13(1):68. doi:10.1186/s40164-024-00529-z
39. Xu X, Piao HN, Aosai F, et al. Arctigenin protects against depression by inhibiting microglial activation and neuroinflammation via HMGB1/TLR4/NF-κB and TNF-α/TNFR1/NF-κB pathways. *Br J Pharmacol*. 2020;177(22):5224–5245. doi:10.1111/bph.15261
40. Sun P, Zhao X, Zhao W, et al. Sophora flavescens-Angelica sinensis in the treatment of eczema by inhibiting TLR4/MyD88/NF-κB pathway. *J Ethnopharmacol*. 2024;322:117626. doi:10.1016/j.jep.2023.117626
41. Wang Z, Zhang H, Qi C, et al. Ursolic acid ameliorates DNCB-induced atopic dermatitis-like symptoms in mice by regulating TLR4/NF-κB and Nrf2/HO-1 signaling pathways. *Int Immunopharmacol*. 2023;118:110079. doi:10.1016/j.intimp.2023.110079
42. Lim JM, Lee B, Min JH, et al. Effect of peiminine on DNCB-induced atopic dermatitis by inhibiting inflammatory cytokine expression in vivo and in vitro. *Int Immunopharmacol*. 2018;56:135–142. doi:10.1016/j.intimp.2018.01.025
43. Shi J, He L, Tao R, et al. TLR4 polymorphisms as potential predictors of atopic dermatitis in Chinese Han children. *J Clin Lab Anal*. 2022;36(5):e24385. doi:10.1002/jcla.24385
44. Gong P, Jia HY, Li R, et al. Downregulation of Nogo-B ameliorates cerebral ischemia/reperfusion injury in mice through regulating microglia polarization via TLR4/NF-κappaB pathway. *Neurochem Int*. 2023;167:105553. doi:10.1016/j.neuint.2023.105553

Drug Design, Development and Therapy

Publish your work in this journal

Drug Design, Development and Therapy is an international, peer-reviewed open-access journal that spans the spectrum of drug design and development through to clinical applications. Clinical outcomes, patient safety, and programs for the development and effective, safe, and sustained use of medicines are a feature of the journal, which has also been accepted for indexing on PubMed Central. The manuscript management system is completely online and includes a very quick and fair peer-review system, which is all easy to use. Visit <http://www.dovepress.com/testimonials.php> to read real quotes from published authors.

Submit your manuscript here: <https://www.dovepress.com/drug-design-development-and-therapy-journal>

Dovepress
Taylor & Francis Group